POLITECNICO DI TORINO

Master's Degree in Mechatronic Engineering

Master's Degree Thesis

Data-based modelling and optimal control for wave energy conversion systems

Supervisors

Prof. Nicolas FAEDO

Prof. Giuseppe GIORGI

Candidate

Bayram KARACA

DECEMBER 2024

Abstract

Wave energy holds great potential as a renewable energy source. To make use of this potential, wave energy converters (WECs) are utilized to capture the perpetual motion of the ocean as an energy source. However, WECs have not reached commercial maturity, marked by significant variability and a lack of standards. Furthermore, improving the efficiency of the wave energy converters is still a key challenge. In order to make it applicable against operational costs, which is a crucial factor for the economical viability of the device, control technology has an major role to play and needs to be further explored and improved. However, the control of WECs differs from the standard control problem, which generally focuses on set-point/reference tracking, and insteads aims for energy maximization. In this thesis, a generalized framework has been developed for the identification and optimization of WEC systems. The framework integrates various tools for the simulation of the underlying system dynamics using so-called hydrodynamic coefficients and for the optimization of power take-off (PTO) trajectories. From system identification to optimization, each stage is included and tailored for compatibility with the pseudo-spectral method, which is used for the discretization of the optimization problem. A set of simulations is carried out to validate the results of the framework in numerous sea states to maximize energy extraction while constraining the PTO motion and force. Two different WEC models were tested, allowing for a comparative analysis of parameter impacts within the framework. The results validate the framework's effectiveness and lay the groundwork for further studies toward developing more practical and cost-effective WEC devices.

Acknowledgements

I am sincerely grateful to Professor Nicolas Ezequiel Faedo and Professor Giuseppe Giorgi for entrusting me with this project and for their invaluable mentorship throughout my journey. Their insights and guidance have been instrumental in shaping this work. I also wish to extend my thanks to the team at the More Energy Lab.

I would like to express my heartfelt gratitude to my parents for their unwavering belief in me and their endless support. Their financial and emotional assistance have been pivotal in my achievement of this degree. I am deeply thankful to my sisters, who motivated me daily and sent their best wishes throughout this journey. Knowing that my family was always just a phone call away during my most challenging moments reminded me that I was never alone.

A special thanks goes to my dear friend Fehmi, whom I consider part of my family. From graduating together to pursuing our master's studies in Italy, we have shared this journey side by side. His unwavering support, encouragement, and ability to ease my worries have been an invaluable source of strength throughout this experience.

Lastly, I would like to thank all my friends who supported me throughout this journey. Their kindness and encouragement have meant so much.

"He who desires but acts not, breeds pestilence."
William Blake, The Marriage of Heaven and Hell

Table of Contents

List of Tables

List of Figures

Acronyms

WEC
: wave energy converter

PTO
: power take-off

DoF
: degree-of-freedom

BEM
: boundary element method

Chapter 1

Introduction

1.1 Context

The world temperature is rising each year, and as industrialization and modernization continue, the need for energy increases. That's why the importance of converting energy production to renewable sources is becoming a more urgent situation every day. The significance of employing renewable energy sources is to diminish the negative impact on nature. Many technologies that claim to be green, such as electric vehicles, rely on electricity that is still heavily dependent on fossil fuels with a 60% rate [1]. Since the onset of industrialization, the Earth's average surface temperature has risen by 1.1 °C as a result of greenhouse gas emissions from fossil fuel consumption. If no regulations are implemented, this temperature difference is anticipated to increase to 2.5 °C by the end of the century [2]. Consequently, the key to reducing the adverse effects of global warming lies in decreasing our dependence on fossil fuels.

Wave energy is one of the many renewable energy sources. There are vast oceans around the world that are nurtured with the blessing of powerful waves formed from solar energy accumulated over huge ranges of water bodies. For example, Western Europe has the potential of 50 kW/m of wave power on its western coast. In total, this amounts to 2 TW, which is equivalent to the world's energy requirements, and it is estimated that up to 25% of this potential can be effectively converted [3]. There are many ways to capture the energy from the waves, as discussed within this monograph in upcoming sections. The main focus of this thesis is on wave energy converters (WECs), which are devices that capture energy from ocean waves. According to the recent research, they currently represent a minor fraction of the energy while having huge potential across the world [4]. This is due to the technical challenges to deployment because of the harsh sea conditions and high initial costs

(h) 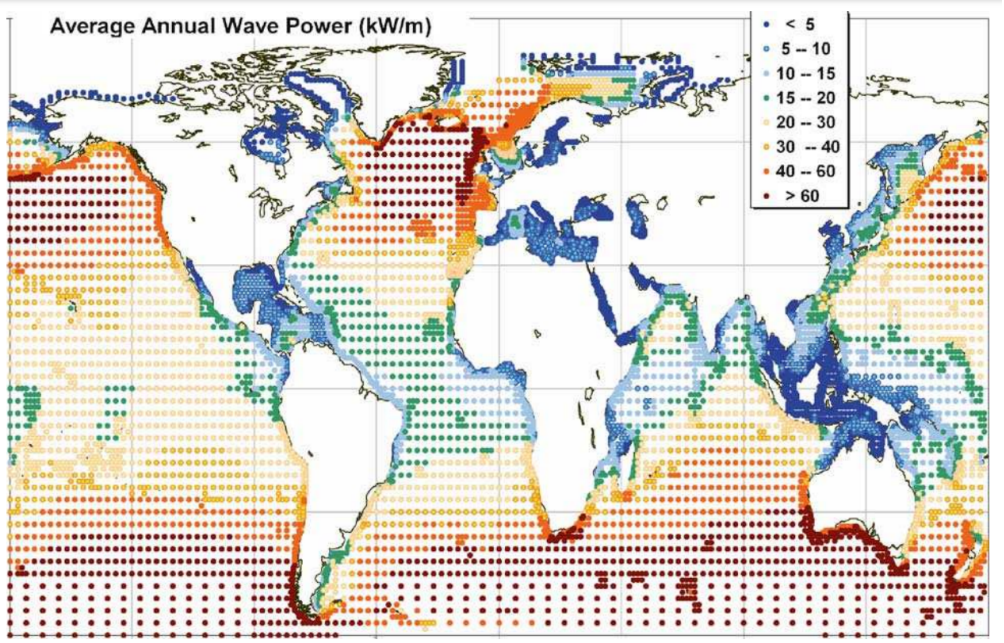

Figure 1.1: Map of average annual wave power [3]

[5]. It is a relatively young research branch, thus the use of this technology is not that widespread, and it is needed to promote it to tap into the vast energy potential held by the ocean waves.

WECs will be reviewed in depth in the theoretical background section. These devices can be initially modelled as mass-spring-damper systems, floating or fixed on the sea base. In order to extract energy, they require a power take-off (PTO) device. By actuating the PTO according to the incoming wave, the potential carried by the wave can be captured. The main working principle of these applications is to exaggerate the motion of the axis where the control of PTO is implemented. The main challenge for these applications is to capture the energy optimally without causing any damage to the operational devices. Operational costs have a big impact too, and the importance of control is indisputable to increase the affordability of the device [6].

1.2 Motivation

In this section, the challenges explained in the background will be addressed, and the motivation of the project will be composed. The main challenges consist of

dependence on fossil fuels and limitations to the use of wave energy effectively. It is necessary to benefit from all kinds of renewable energy sources, and wave energy is no exception. Therefore, it is important to develop such systems that convert the energy caused by the constant wave motions around the world. While the research on other renewable energy sources like solar energy or wave energy has matured over the years, there is still a need to do research on WEC systems, and it is necessary to fill the possible research gaps [7]. By ensuring more effective control, operational costs can be minimized. For this, it is essential to work on control systems that are accessible and standardized. As a solution, a versatile framework containing many tools can be developed. It should also approach the control problem of the WEC by tailoring it into a standardized form.

It is essential to develop a robust framework capable of identifying WEC dynamics and optimizing WEC performance. In this thesis, the framework is designed in a way that all the processes are repeatable and parametrized for convenience. Two different WEC models will be analyzed, and the results will be compared. The focus will be on a single degree of freedom (DoF), but extensions to multiple DoFs will be addressed. In the framework developed, the desired control trajectory is obtained with a force input and using non-parameterized impedance data. (e.g., force, pos, acc, etc.). Maximum efficiency and performance are important to use the most of the potential from the wave excitation.

There is a lot of variety in the industry of ocean engineering and WEC designs, and the researchers don't use standardized methodology on many occasions. It is crucial to alleviate the complexity of navigating different techniques, configurations, and modes of control. The framework should have the capability to handle differently configured systems. This way, distinct systems can be compared with the outputs, like power matrices, which can show the efficiency of the application and used as a performance criterion. Then again, to ensure user-friendliness, the framework should be operable with a single file. The ease of implementation could facilitate widespread adoption of the framework.

A cohesive system is envisioned where only the geometry input is required to carry out all stages of analysis without considering the configuration of WEC. Although the analysis will focus on linear systems, the framework will be designed to allow for future extensions, such as incorporating nonlinear features. The primary objective is to develop a system capable of delivering quick results with a short processing time. Working in the runtime is not the current goal, but in future works it can be adapted. Integration with different control types should be easy to implement. Various dynamics should be utilized, such as PTO dynamics.

1.3 Objective

To understand the working principle of wave energy systems, comprehensive background research will be carried out. A standardized method will be applied to accommodate the diversity of the WEC types. The framework will focus on single-body and single degree-of-freedom (DoF) configurations, aiming to provide tools for both system identification and control optimization. This scalable framework will incorporate non-parametric identification and pseudo-spectral methods to address identification and energy maximization, respectively. Identification and energy maximization methods will be addressed with non-parametric identification and pseudo-spectral methods, respectively. The device will be simulated in different working conditions, such as multidirectional waves or irregular waves.

This application will be implemented in a way that it will not require much processing power and will quickly provide us with ready-to-implement results since minimization of runtime is an important task as the simulation times can go out of hand quickly. Another aspect of the framework will be ensuring that the applied forces and operating conditions do not adversely affect the device's health, aiming to maximize the device's lifespan.

The work will serve as groundwork for future studies. So it needs to be open to development, repeatable, parameterizable, automatic, and easy to implement. Another trait would be monitoring of all the possible stages of the application; thus, it needs to be trackable and suitable for reporting. It shouldn't have a complex interface. It should have a validation mechanism as an extra to troubleshoot the possible problems. In this way, with the form of a framework that has a simple and quick solution, it will lay the groundwork for a preliminary study of the development of techno-economic analysis of WEC systems.

1.4 Outline

From the provided background, motivation, and objectives, it is decided to implement the following approach. WECSim will be utilized to simulate various sea conditions for linear WEC systems. It will also serve as a versatile tool for implementing control methods and a crucial resource for validating outcomes. WecOptTool will be used for the optimization. Optimization results from WecOptTool will then be imported back into WECSim to ensure consistency between the simulations, thereby establishing a coupling between these two distinct software tools. Since WECSim is based on MATLAB, many processes will be handled with MATLAB, and the data will be tailored for the optimization stage. This includes

tasks such as system identification and the estimation of wave excitation forces, all conducted in a non-parametric manner. This data-driven identification approach leverages the pseudo-spectral method.

This thesis is structured into 5 chapters. **Chapter 1** gives context for the thesis subject, explains the motivations and objectives, and outlines the overall structure of the thesis. **Chapter 2** deals with the theoretical background of the WECs by delving into their classification, modeling, control techniques, and scaling and explains the tools utilized in the framework. **Chapter 3** explains the methodology used for this work, including identification, excitation force estimation, filtering, optimization, and mentions the possible extensions for the framework. **Chapter 4** presents the results for two different WEC models, allowing a comparative analysis. **Chapter 5** draws a conclusion for the work carried out and mentions the future works.

Chapter 2

Theoretical Background

This section covers the essential theoretical concepts. The first section gives the important info about **Wave Energy Converters**. **Potential Flow Theory** section explains the body-wave interactions. **Hydrodynamic Modeling** section captures the system dynamics by introducing each element of the Cummins' equation. **Cummins' Equation** section shows the derivation of Cummins' equation from the potential flow theory. **Control Strategy in WEC Systems** section explores different control technologies employed for WECs. **Pseudo-spectral Method** section gives the theoretical background about the optimization problem. In the last two sections,**WECSim** and **WecOpt** are introduced.

2.1 Wave Energy Converters (WEC)

WECs are designed to capture wave energy, typically induced by wind-driven ocean waves [9]. In this section, WEC systems will be discussed by showing the proposed model schemes, and classification of these systems will be carried out. The history of WECs dates back to a device patented in 1799 [10]. A lot of different models of WECs advanced since then and it gained the popularity after the global awareness of climate change increased significantly during the 1970s [11]. There is a lot of variety in the wave energy technologies because of the methods to absorb energy depending on the water depth and the location [8].

The main challenges in the design of WECs are having an economically viable system and adapting to the various conditions of the sea, such as irregularity of waves in terms of amplitude, phase, and direction, or severe conditions like storms or hurricanes [12]. Being adaptable to severe conditions causes an immense increase in the budget. These conditions affect the reliability of the device as well, causing a decrease in the performance over time. Thus, considering real-life conditions in the

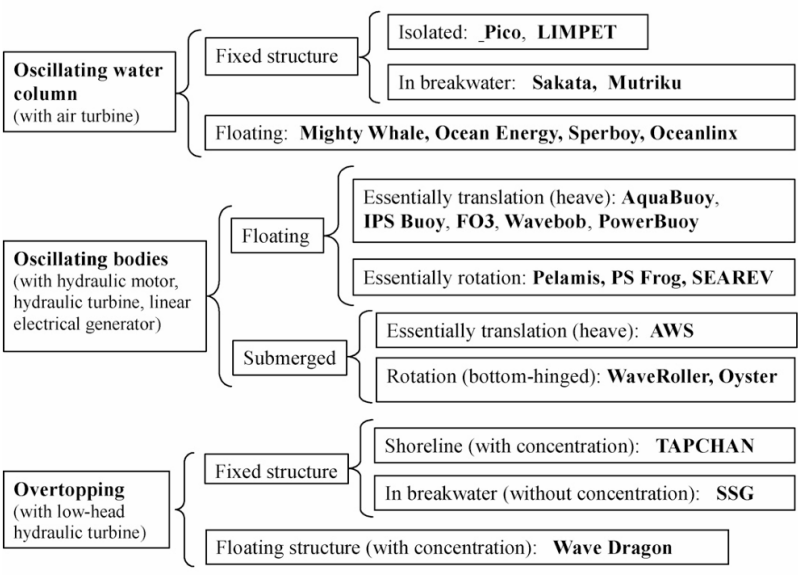

Figure 2.1: Classification of Wave Energy Converters [8]

design process will make the system more robust against the decline of reliability. In the literature, there are a lot of WEC types finding solutions to the various problems mentioned here.

There are three main types of wave energy converters according to their principle of operation as shown in fig. 2.1. These are oscillating water columns, oscillating bodies, and overtopping devices. In the thesis, oscillating bodies will be put in the focus. The other two types of wave energy converters will be explained shortly to help understand better how the different techniques are utilized. Alternative classifications take into account the deployment site and the type of PTO utilized as a generator. However, to maintain the self-contained focus of this thesis, these classifications will not be reviewed.

2.1.1 Oscillating Water Column WECs

Oscillating water column devices consist of a partially submerged solid structure that is open beneath the water surface. Above the water's surface, internal air is trapped. Through an axial flow turbine, air flows as a result of the wave's oscillation [8]. The principle of working of these devices can be seen in fig. 2.2.

As a fixed configuration, a few full-sized projects are deployed in open coastal waters. They are called first generation and deployed close to shore for easier

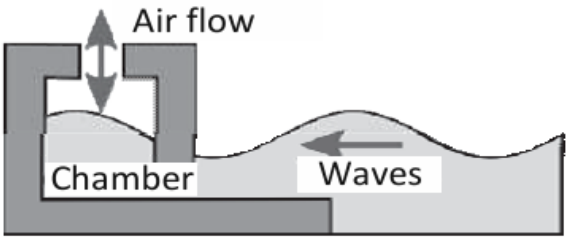

Figure 2.2: Oscillating Water Column WECs [13]

installation [8]. They are connected to the sea base without the need for long wires to carry the electricity ashore. Yoshio Masuda had a lot of contributions to the advancement of these technology especially with the 80 m x 12m x 5.5 OWC prototype called Kaimei built in 1978 (fig. 2.3). This device had 5 air turbines each having 125 kW rating [14].

Figure 2.3: Kaimei [14]

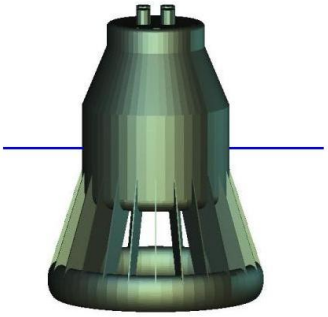

Figure 2.4: SPERBOY [15]

As a floating configuration, SPERBOY (shown in fig. 2.4) is developed by Embley energy. The generators inside of the device make use of the air moved by the oscillation of the water surface [15]. The floating OWC devices can also benefit from the free oscillation of the body if they are designed with this goal [8].

2.1.2 Overtopping WECs

Overtopping wave converters (fig. 2.5) operate by harnessing the gravitational potential energy of seawater that flows to elevated levels after wave crests' collision with the WEC body [8]. The seawater then spills into a chamber which has a low-head hydraulic turbine inside. One of the best example of this type of WEC is Wave Dragon (shown in fig. 2.6) and earliest implementations of the overtopping

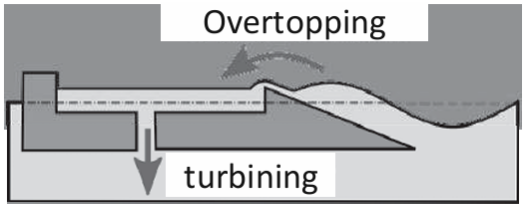

Figure 2.5: Overtopping WECs [13]

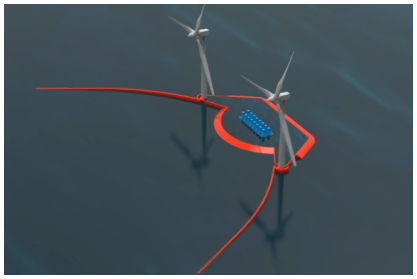

Figure 2.6: Wave Dragon [16]

concept is the Tapchan (Tapered Channel) system, which utilizes a reservoir where the overtopped water is collected.

2.1.3 Oscillating Body WECs

Oscillating body WEC operate offshore to capture wave energy thorough the motion of floating or submerged structures[8]. These systems can be categorized into single-body, two-body and multi-body configurations, each offering unique mechanisms and challenges.

Oscillating body WEC is a complex configuration requiring mooring and maintenance, causing challenges to full embrace of this technology. The simplest design is a single-body configuration named point absorbers, which has a motion of up and down relative to a fixed frame of reference. Their diameter is much smaller than the wavelength of the sea. Corpower's WEC is a great example of this configuration which is shown in fig. 2.7.

Figure 2.7: Corpower's WEC [17]

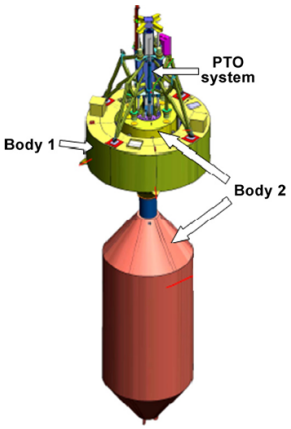

Figure 2.8: Wavebob WEC [8]

Single-body WECs have a disadvantage related to sea level, which is not always the same because of the tidal movements, making a seafloor-attached system impractical [8]. Instead, a two-body configuration can be used to leverage the relative motion between the two bodies as shown in fig. 2.8 which is a prototype of this kind of configuration.

Figure 2.9: Wave Star [18]

Multi-body systems comprise several floating point absorbers linked to a fixed structure and PTO system. These bodies oscillate in relation to a common reference frame to produce energy. Danish Wave Star (shown in fig. 2.9) is one of the best examples, which comprises two linear arrays of floaters situated on either side of a stationary steel structure oriented with the principal wave direction.

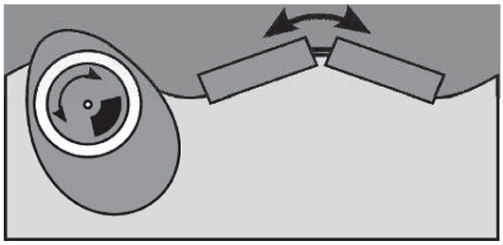

Figure 2.10: Pitching WECs [13]

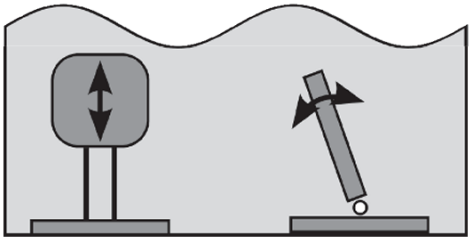

Figure 2.11: Submerged WECs [13]

WECs can capture the energy from different modes of motion too. For example, pitching devices utilize pitch motion. Relative angular movement of floating bodies is used to generate power in these systems shown in fig. 2.10. Some bottom-hinged WECs can make use of the pitch motion to capture energy, as can be seen in fig.

2.11. They consist of two bodies, one hinged to the seabed and the other a flap-like structure that swings back and forth with the interaction of an incident wave.

2.2 Potential Flow Theory

Potential flow theory serves as a foundational approach to understanding hydrodynamic interactions between WECs and small-amplitude waves. The theory considers an ideal flow, which is frictionless, irrotational, and incompressible. The assumption for inviscid or frictionless flow can be invalid when the waves are large. This kind of situation can induce immense nonlinearity during the calculation of wave-body interactions. Each of the technical terms will be explained in this section.

2.2.1 Irrotational Flow

Irrotational Flow is explained briefly as follows. A fluid particle moving without rotation will not develop a rotation under the action of a body force or a normal surface pressure force. Rotation requires a shear stress and thus angular deformation. The presence of viscous forces means the flow is rotational. This assumption can become applicable further away from the boundary layers near the solid surfaces. Formally, this can be written in terms of the following condition:

$$\nabla \times \vec{V} = 0, \tag{2.1}$$

where $\vec{V}$ is the velocity vector, ∇ indicates the gradient operator.

2.2.2 Velocity Potential

Velocity Potential, Φ is used to describe the flow field of an incompressible and irrotational fluid, i.e taking the gradient of the velocity potential $\Phi = \Phi(x, y, z, t)$, which is 3-dimensional and time dependent, the velocity vector $\vec{V} = (u, v, w)^T$ can be calculated as

$$\vec{V} = \nabla\Phi. \tag{2.2}$$

2.2.3 Laplace Equation

Laplace Equation is derived which is the basis of the potential flow theory using the explained notions previously. **Ideal flow** is incompressible and inviscid (irrotational). Thus incompressibility can be realized with the continuity equation:

$$\textbf{Continuity: } \nabla \cdot \vec{V} = 0. \tag{2.3}$$

while irrotationality can be written as

$$\textbf{Irrotational: } \nabla \times \vec{V} = 0 \quad \Rightarrow \quad \vec{V} = \nabla\Phi. \tag{2.4}$$

If the irrotationality condition is substituted in the continuity equation, the Laplace equation is derived as follows:

$$\nabla \cdot \vec{V} = \nabla \cdot (\nabla\Phi) = \nabla^2\Phi = \frac{\partial^2\Phi}{\partial x^2} + \frac{\partial^2\Phi}{\partial y^2} + \frac{\partial^2\Phi}{\partial z^2} = 0. \tag{2.5}$$

2.3 Hydrodynamic Modeling

As illustrated within fig. 2.12, the total forces on the WEC body are categorized as external forces and reaction forces [19]. External forces occur because of the interaction of the body with water. These include hydrostatic and hydrodynamic forces, which can be further divided into excitation and radiation forces. Hydrostatic force stands for the buoyancy from Archimedes' law. The displacement of mass in the water causes radiation forces. Excitation forces occur mostly from the wave-body interactions and include Froude-Krylov and diffraction forces. Froude-Krylov effects depend on the change of the wetted area of the body. Diffraction effects caused by the collision of the wave and body thus causing new oscillations. All of these forces will be explained in detail in the following subsections.

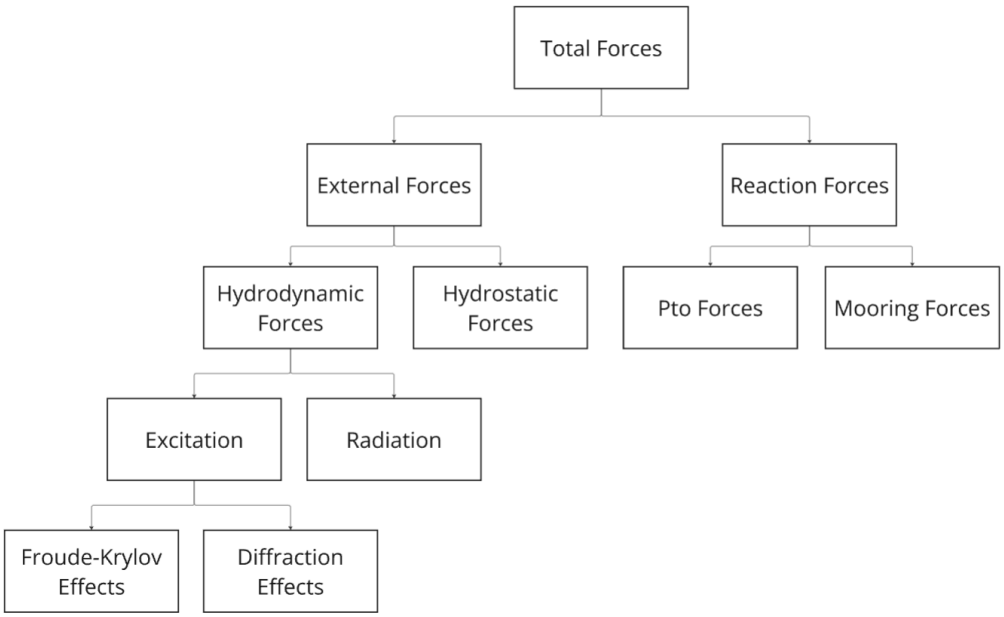

Figure 2.12: Decomposition of Forces Acting on WEC

The main forces comprising the loads on the WEC body are:

$$m\ddot{\zeta} = f_{hs}(\nu) + f_{fk}(\nu, \zeta) + f_d(\nu) + f_r(\zeta) + f_v(\dot{\zeta}) - f_u \tag{2.6}$$

where m is total inertia, $\zeta(t)$ is displacement, $\nu(t)$ is wave elevation, f_{hs} is the hydrostatic force, f_{fk} is the Froude-Krylov force, f_d is the diffraction force, f_r is the radiation force, f_v is the viscous force and, finally, f_u represents the control force.

2.3.1 Hydrostatic Forces

Hydrostatic Force is caused by the variation of hydrostatic pressure distribution on the body due to the oscillatory motion of the captor [19]. In other words, it results from the balance between buoyancy and gravity, expressed as:

$$f_{hs} = -G\zeta \tag{2.7}$$

where G is the hydrostatic spring stiffness.

2.3.2 Hydrodynamic Forces

Excitation Loads occur due to the action of incident waves on a motionless captor [19]. The waves encounter a vessel to be at rest, which experiences a time-dependent force, caused by the changing pressure field. It consists of two forces which are FK forces and diffraction forces.

$$F_e = f_{fk} + f_d \tag{2.8}$$

where f_{fk} is derived from the velocity potential of the undisturbed incident wave, considering the pressure distribution over the mean wetted surface of the motionless body, f_d is the scattering component of the excitation force, resulting from the integration of the scattered wave potential over the mean wetted surface.
Diffraction force for the input $\eta(t)$ is calculated in eq. 2.9.

$$f_d(\eta) = k_d * \eta \tag{2.9}$$

where k_d is impulse response.
Radiation Force is the force experienced by the captor due to the pressure field alteration as a result of the fluid displaced by its oscillatory movement in an incident wave field [19]. It can be expressed as:

$$f_r = -m_\infty \ddot{z} - k_r * \dot{z} \tag{2.10}$$

where m_∞ added mass at infinite frequency, k_r is the radiation impulse response function.

2.3.3 Reaction Forces

Reaction forces consists of the inner forces applied by the wec device and consists of PTO force, Mooring Force and Endstop. **Power Take-off (PTO)** converts mechanical energy into electricity or another useful energy vector. **Mooring System** is responsible for station keeping.

2.4 Cummins' Equation

To understand the connection between potential flow theory and the dynamics of Wave Energy Converters (WECs), it is essential to consider the underlying equations governing the flow. In particular, the flow must satisfy both Laplace's equation and Bernoulli's equation on the sea surface for a proper formulation of WEC dynamics. The hydrodynamic force acting on a floating body is derived from the dynamic pressure integrated over the mean wetted body surface, S_b [19]. To explore the concept of dynamic pressure, we begin with **Bernoulli's equation** for unsteady flows.

2.4.1 Dynamic Pressure from Bernoulli's Equation

The dynamic pressure p_e due to unsteady flow can be expressed as:

$$p_e = -\frac{1}{2}\rho\left(\nabla\Phi\right)^2 - \rho\frac{\partial\Phi}{\partial t} \tag{2.11}$$

where ρ is the fluid density and Φ is the velocity potential. For large wavelength waves, the quadratic terms become negligible, and we can simplify the equation by ignoring the second-order terms. Thus, the dynamic pressure becomes:

$$p_e = -\rho\left(\frac{\partial\Phi}{\partial t}\right) \tag{2.12}$$

2.4.2 Hydrodynamic Force on a Floating Body

The linear hydrodynamic force acting on a floating body is then obtained by integrating the dynamic pressure over the wetted body surface [19], S_b:

$$\hat{F}_e = \int_{S_b} p_e\,\mathbf{n}\,dS_b = \int_{S_b}\left(-\rho\frac{\partial\Phi}{\partial t}\right)\mathbf{n}\,dS_b \tag{2.13}$$

where $\mathbf{n}$ is the unit vector normal to the body surface, and Φ is the total velocity potential.

2.4.3 Total Velocity Potential

The total velocity potential Φ acting on the body can be expressed as the sum of three components:

$$\Phi = \Phi_0 + \Phi_s + \Phi_r \tag{2.14}$$

where Φ_0 is the incident wave potential, Φ_s is the scattered potential, and Φ_r is the radiation potential [19]. Substituting this into the expression for the hydrodynamic force, we get:

$$\hat{F}_e = i\omega\rho \int_{S_b} (\Phi_0 + \Phi_s + \Phi_r)\, \mathbf{n}\, dS_b \tag{2.15}$$

where ω is the angular frequency of the incident waves.

2.4.4 Linearized Force and Cummins' Equation

When considering a linearized version of these forces, we arrive at **Cummins' Equation**, which is widely used in the literature for modeling the dynamics of floating bodies under wave excitation:

$$(M + A^0)\ddot{z}(t) + \int_0^t K(t-\tau)\dot{z}(\tau)\, d\tau + C \cdot z(t) = F_{\text{wav}} - f \tag{2.16}$$

In Cummins' Equation, various parameters play a crucial role in defining the motion of a floating body under wave excitation. The term M represents the mass of the body, while A^0 is the added mass matrix, which accounts for the inertia of the displaced fluid. The function $K(t-\tau)$ is the radiation impulse response function, capturing the effect of wave radiation on the body's motion. The restoring coefficient C defines the restoring forces arising from buoyancy and elasticity, while $z(t)$ denotes the vertical displacement of the body. The total wave excitation force, denoted F_{wav}, consists of the diffraction force F_d and the force due to the incident wave field F_{FK}. Lastly, the external force f represents any additional forces acting on the body, such as damping or control forces.

Moreover, Cummins' Equation provides a time-domain representation of the motion of floating bodies under wave excitation, incorporating both linear and radiation forces. It is a critical equation in the modeling and simulation of WEC systems, allowing for the prediction of the body's dynamic response to wave forces.

2.5 Control Strategy in WEC Systems

The marine industry depends on the safety of the devices deployed because of the harsh nature of the ocean [20]. It is important to regulate the control of WECs against extreme conditions of the sea. So, every control method should prioritize

the health of the device while minimizing maintenance frequency, and of course doing all of these in an economically efficient sense. Thus, the control strategy of WEC systems is a non-standard one since it requires energy maximizing in safe operation limits rather than set point tracking [21].

In this section, the main control strategies in the current literature will be presented as suboptimal and optimal control types.

2.5.1 Suboptimal Control Types

Suboptimal control types include damping, reactive, impedance matching and latching control. They are discussed in the following paragraphs in order by showing the related equations and explaining the concepts.

Damping control (eq. 2.17) is also called resistive control. It is the simplest control structure which depends on velocity of the device [20], i.e.

$$f_{pto}(t) = -B_{pto}v(t). \tag{2.17}$$

The PTO force is applied proportional to the PTO velocity to damp the system more when it oscillates faster [22]. The parameter in relation here is the damping coefficient, which can be calculated easily in the regular waves but not in the irregular wave environment. This is because of the radiational damping of the device is not constant with respect to the irregular waves.

Reactive control (eq. 2.18) advances the concept of damping control by adding an integral term, which is the reactance (depends on the position of the device) [22]. Unlike the damping control, this time PTO can work in motor mode too. In these control methods, the PTO force is calculated with the spring coefficient and damping coefficient, which are dependent on position and the velocity of the PTO, i.e.

$$f_{pto}(t) = -B_{pto}v(t) - K_{pto}x(t) \tag{2.18}$$

These coefficients should be tuned according to sea conditions with the constraints of pto force and displacement.

Impedance-matching control (fig. 2.13) Control system designed leveraging this technique aim at matching the impedance of the PTO with the intrinsic impedance of the WEC body. It is done by applying the complex-conjugate of the intrinsic impedance as shown in the figure [23]. Note that, in fact, both damping and reactive controllers are a subset of impedance-matching based techniques, since their effective tuning is performed leveraging the very same optimality conditions.

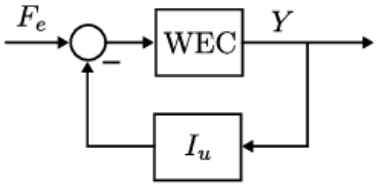

Figure 2.13: Impedance-matching Control [24]

Latching control is another type of suboptimal method that is not using the PTO in motor mode thus it doesn't transfer energy back to the waves. During the wave oscillation, the device body is hold and released to increase the oscillation speed [20]. In this method, the most important point is to find the best latching/unlatching periods with respect to sea conditions.

2.5.2 Optimal Control Types

Optimal control for WECs are virtually always included within the family of direct optimal control methods, where the (infinite-dimensional) optimal control problem is discretised and solved numerical. This includes, for instance, pseudo-spectral methods, and MPC-like controls. In general, optimal methods depend on the future forecast of the wave information; thus, these are intrinsically non-causal. In this part each of these techniques are presented briefly.

The pseudo-spectral method uses a mathematical method in which the control problem is divided into smaller, manageable subproblems within a limited time horizon. By separating the behavior of a system into its spectral components. This method effectively handles constraints such as PTO force or displacement limits. Accurate optimization within operating limits is especially effective in demanding systems.

Model Predictive Control (MPC) works by continuously predicting the future state of the system based on dynamic models and incoming wave data [23]. in each step the control inputs are optimized to achieve maximum energy removal. while adhering to safety and operational constraints.

MPC is ideal for complex systems that have many restrictions. This is because it is a structured way to balance energy extraction and operational safety. while still requiring large amounts of computational resources. Finding real-time solutions can be challenging for non-linear or highly convex optimization problems. In practical applications, a simpler version of MPC is often used to balance computational feasibility with performance.

These optimal control strategies excel in environments where precise control limits and energy efficiency are critical.

2.6 Pseudo-Spectral Method

One popular direct transcription method for resolving optimal control issues is the pseudo-spectral method. This approach is notable for its computational effectiveness, particularly when working with intricate systems. Given that it supports multi-body and multi-DoF devices, its use in WEC optimization is beneficial. The pseudo-spectral approach allows formulating constrained problems, allowing bounds on both the motion and the PTO force.

The discretization process is customized for generic WEC configurations and uses flexible sets of basis and test functions. A thorough derivation of the quadratic program is provided to make solving these issues easier [21]. In a particular function space, any function in the WEC model may be mathematically expressed as a linear combination of these base functions. The weighted average residual formulation is used to handle the restrictions in WEC systems. With this method, system dynamics can be accurately represented and controlled under a range of operational limitations.

Objective function used for the power maximization is

$$J = -\int_0^T \dot{z}(t) f_{\text{pto}}(t)\, dt \tag{2.19}$$

where $\dot{z}$ is the device heave velocity, f_{pto} is the PTO force.

System Dynamics can be represented with the classic Cummins' equation, i.e.

$$M\dot{x}_2 = -Bx_2 - \int_{-\infty}^{t} K(t-\tau)x_2(\tau)\, d\tau - Sx_1 + u + f_e \tag{2.20}$$

where M is inertia consisting body mass and added mass, B is linear damping, S is hydro-static stiffness, u is control input, f_e is wave excitation and the integral term is used for the calculation of radiation damping.

In order to enforce the system dynamics, it is going to be converted to residual form as $r = ma - \sum f$ and this residual value will be minimized in the optimization problem. Other constraints is put on PTO force and device position:

$$|f_{\text{pto}}(t)| \leq F_{\max}, \tag{2.21}$$

$$|z(t)| \leq Z_{\max} \tag{2.22}$$

It is needed to approximate the system states such as x_1, x_2 and f_{pto} to apply direct transcription method. This is done by choosing Fourier series as basis functions:

$$x_i(t) \approx \sum_{k=1}^{N/2} x_{ik}^c \cos(k\omega_0 t) + x_{ik}^s \sin(k\omega_0 t) = \Phi(t)\hat{\boldsymbol{x}}_i, \tag{2.23}$$

$$u(t) \approx \sum_{k=1}^{N/2} u_k^c \cos(k\omega_0 t) + u_k^s \sin(k\omega_0 t) = \Phi(t)\hat{\boldsymbol{u}}, \tag{2.24}$$

$$\Phi(t) = \left[\cos(\omega_0 t), \sin(\omega_0 t), \ldots, \cos\left(\frac{N}{2}\omega_0 t\right), \sin\left(\frac{N}{2}\omega_0 t\right)\right]^\intercal \tag{2.25}$$

where $\Phi(t)$ is truncated Fourier series array.

Objective Function takes the following form after the direct transcription:

$$J^N = -\int_0^T \hat{\boldsymbol{u}}^\top \Phi^\top(t)\Phi(t)\hat{\boldsymbol{x}}_2 \, dt = -\frac{T}{2}\hat{\boldsymbol{u}}^\top \hat{\boldsymbol{x}}_2 \tag{2.26}$$

while the system dynamics can be written as:

$$\begin{aligned} M\Phi(t)\boldsymbol{D}_\phi\hat{\boldsymbol{x}}_2 = -B\Phi(t)\hat{\boldsymbol{x}}_2 - \int_{-\infty}^{t} K(t-\tau)\Phi(t)\hat{x}_2(\tau)\, d\tau \\ - S\Phi(t)\hat{\boldsymbol{x}}_1 + \Phi(t)\hat{\boldsymbol{u}} + f_e \end{aligned} \tag{2.27}$$

where $\boldsymbol{D}_\phi$ is differentiation matrix which is the derivative of zero mean Fourier series, i.e.

$$\boldsymbol{D}_\phi = \begin{bmatrix} 0 & k\omega_0 \\ -k\omega_0 & 0. \end{bmatrix} \tag{2.28}$$

where $k = 1, ..., N/2$. Note that is invertible and one of the strong points of these method because it simplifies the differentiation process.

The discretized constraints can be written in an analogous form, i.e.

$$|\Phi(t)\hat{\boldsymbol{u}}| \leq F_{\max}, \tag{2.29}$$

$$|\Phi(t)\hat{\boldsymbol{x}}_1| \leq Z_{\max} \tag{2.30}$$

After the discretization process is carried out, it is evident that the problem is generalized, with the overall dynamics converted into the following linear expression:

$$\bar{\boldsymbol{I}}\hat{\boldsymbol{x}}_2 = \hat{\boldsymbol{u}} + \hat{\boldsymbol{e}}. \tag{2.31}$$

In this equation $\bar{\boldsymbol{I}}$ coincides to parametric impedance which will be identified in this thesis in a non-parametric way.

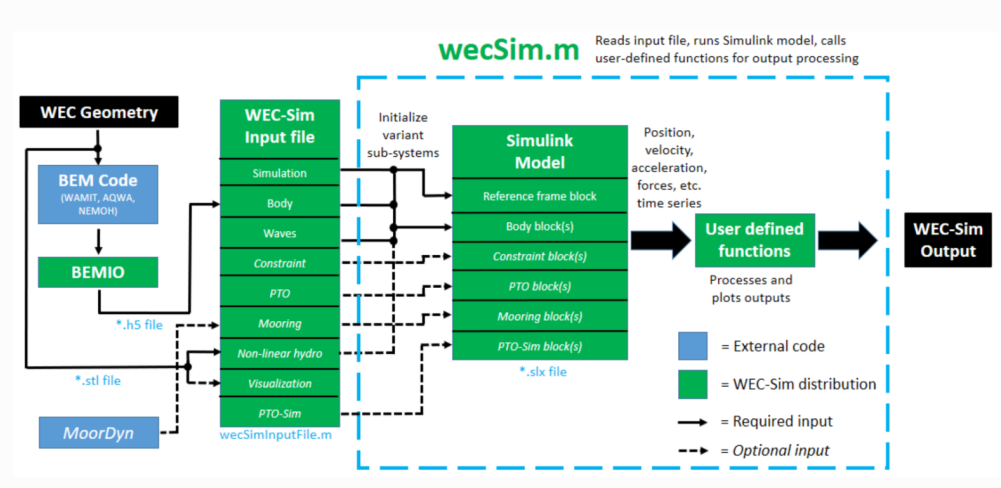

Figure 2.14: WECSim Workflow [25]

2.7 WECSim

The workflow of WECSim is shown in fig. 2.14. As it is covered before in the previous parts, the Cummins' equation is the sole formula that WECSim uses for the simulation of the WEC systems, modeling the dynamic response of the device to wave forces. WECSim is very important for the thesis work since the data exported from the simulations in this tool will be used in identification and the optimization stages of the WEC model. WECSim has the capability to work in different wave conditions, like regular waves and irregular waves [25]. It can simulate irregular waves using JONSWAP and Pierson-Moskowitz spectra or can import wave elevation data from time series. It works with the frequency response data, which is taken from the boundary element method (BEM) solver solutions.

BEM solvers work on the principle of linear potential theory, which has the assumption for the flow to be inviscid, incompressible, and irrotational. These methods are utilized to solve the diffraction and radiation forces absorbed by the body surface as a result of changing wetted surfaces. The frequency data taken from the BEM solvers like WAMIT, AQWA, NEMOH, or Capytaine is converted into a new data structure that is in the h5 format to be used in WECSim. This conversion is done using the 'bemio.m' file in the WECSim. It has the capability to solve the impulse response function for the radiation.

The result of the WECSim simulation is in the time domain, so it's convenient to check the transient response. WECSim uses the MATLAB/Simulink environment, which is a strong engineering tool regularly used by the academics. It is a huge plus

to use the power of visual programming in Simulink. Moreover, WECSim solves the multibody dynamics problem using Simscape Multibody, which is a library of Simulink, and it is more intuitive to attach the elements comprising the WEC.

2.8 WecOpt

In this section, WecOptTool is introduced, which is a tool for WEC control based on the pseudo-spectral method.

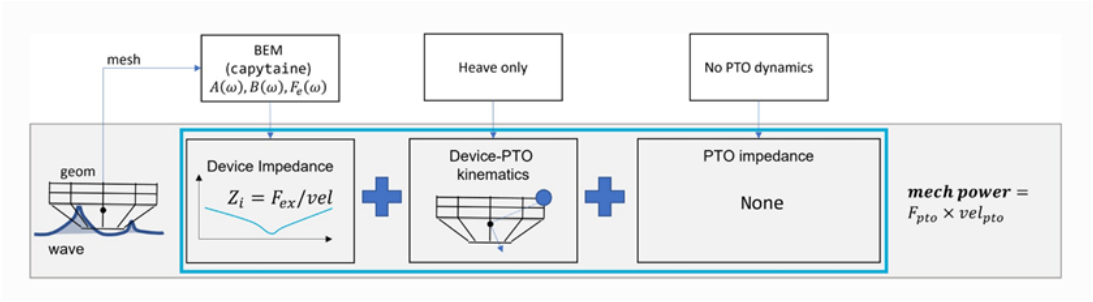

Figure 2.15: WecOptTool Workflow [26]

2.8.1 Workflow

The WecOptTool workflow for a single-body, heave-only WEC, referred to as Wavebot, is illustrated in fig. 2.15. In this example, no PTO dynamics are considered, and the objective is mechanical energy maximization. As can be seen, a BEM solution for the geometry is required. Using the `run_bem()` method, one can achieve this in this framework without the need for external solutions. This method requires a mesh of the geometry, a list of frequencies for which the calculation will be made, gravity, etc. Since the identification process will be used to capture the accurate dynamics of the device, the coefficients related to impedance should be imported externally; thus, there is no need to carry out a BEM solution within this framework.

2.8.2 WEC Object Creation

The hydrodynamic coefficients can be imported by either filling in the properties of WEC directly into the `WEC` object or using a method called `from_impedance()` [26]. The parameters of the `WEC` object can be seen in fig. 2.16. Defining every parameters manually can be an exhaustive task. The second option, the `from_impedance()` method (shown in fig. 2.17), requires only fourier coefficients of the impedance

of the WEC, fourier coefficients of the wave excitation transfer function, linear hydrostatic stiffness, and constraints.

Parameters:

- **f1** (*float*) – Fundamental frequency `f1` $[Hz]$.
- **nfreq** (*int*) – Number of frequencies (not including zero frequency), i.e., `freqs = [0, f1, 2*f1, ..., nfreq*f1]`.
- **forces** (*Mapping[str, StateFunction]*) – Dictionary with entries `{'force_name': fun}`, where `fun` has a signature `def fun(wec, x_wec, x_opt, waves):`, and returns forces in the time-domain of size `(2*nfreq+1, ndof)`.
- **constraints** (*Iterable[Mapping] | None*) – List of constraints, see documentation for `scipy.optimize.minimize()` for description and options of constraints dictionaries. If `None`: empty list `[]`.
- **inertia_matrix** (*ndarray | None*) – Inertia matrix of size `(ndof, ndof)`. Not used if `inertia_in_forces` is `True`.
- **ndof** (*int | None*) – Number of degrees of freedom. Must be specified if `inertia_in_forces is True`, else not used.
- **inertia_in_forces** (*bool | None*) – Set to True if inertial "forces" are included in the `forces` argument. This scenario is rare. If using an intrinsic impedance, consider initializing with `wecoptool.core.WEC.from_impedance()` instead.
- **dof_names** (*Iterable[str] | None*) – Names of the different degrees of freedom (e.g. `'Heave'`). If `None` the names `['DOF_0', ..., 'DOF_N']` are used.

Figure 2.16: Parameters of WEC object

Creating the `WEC` object using the `from_impedance()` method is a better option since it is planned to use data from WECSim to formulate the optimization problem.

The impedance complex coefficients and the complex coefficients of the transfer function, which relate the wave excitation force to the wave elevation, must be imported in a specific data structure to be compatible with the software. This data structure, shown as `exc_coeff()`, should be created in the format shown in fig. 2.18 using the xarray library to enable its use with the `from_impedance()` method.

wecopttool.WEC.from_impedance

static WEC.from_impedance(freqs, impedance, exc_coeff, hydrostatic_stiffness, f_add=None, constraints=None, min_damping=1e-06) [source]

Create a WEC object from the intrinsic impedance and excitation coefficients.

The intrinsic (mechanical) impedance $Z(\omega)$ linearly relates excitation forces $F(\omega)$ to WEC velocity $U(\omega)$ as $ZU = F$. Using linear hydrodynamic coefficients, e.g. from a BEM code like Capytaine, the impedance is given as $Z(\omega) = (m + A(\omega)) * i\omega + B(\omega) + B_f + K/(i\omega)$. The impedance can also be obtained experimentally. Note that the impedance is not defined at $\omega = 0$.

Parameters:
- **freqs** (*ArrayLike*) – Frequency vector $[Hz]$ not including the zero frequency, `freqs = [f1, 2*f1, ..., nfreq*f1]`.
- **impedance** (*DataArray*) – Complex impedance of size `(nfreq, ndof, ndof)`.
- **exc_coeff** (*DataArray*) – Complex excitation transfer function of size `(ndof, nfreq)`.
- **hydrostatic_stiffness** (*ndarray*) – Linear hydrostatic restoring coefficient of size `(ndof, ndof)`.
- **f_add** (*Mapping[str, StateFunction] | None*) – Dictionary with entries `{'force_name': fun}`, where `fun` has a signature `def fun(wec, x_wec, x_opt, waves):`, and returns forces in the time-domain of size `(2*nfreq, ndof)`.
- **constraints** (*Iterable[Mapping] | None*) – List of constraints, see documentation for `scipy.optimize.minimize()` for description and options of constraints dictionaries. If `None`: empty list `[]`.
- **min_damping** (*float | None*) – Minimum damping level to ensure a stable system. See `wecopttool.check_impedance()` for more details.

Raises: ValueError – If `impedance` does not have the correct size: `(ndof, ndof, nfreq)`.

Return type: WEC

Previous Next

Figure 2.17: from_impedance Method

2.8.3 Optimization Problem

Optimization problem is formulated in WecOptTool as follows.

$$\begin{aligned} \min \quad & J(x) \\ \text{subject to} \quad & r(x) = 0 \\ & c_{\text{ineq}}(x) \leq 0 \\ & c_{\text{eq}}(x) = 0 \end{aligned}$$

The objecive fucntion J is the total absorbed energy as shown in eq. 2.32.

$$J = -\int_0^T \dot{\boldsymbol{\eta}}(t)^{\mathrm{T}} \boldsymbol{F}_P \boldsymbol{f}_{\text{pto}}(t) dt. \tag{2.32}$$

```
<xarray.DataArray (omega: 10, wave_direction: 1, influenced_dof: 1)> Size: 160B
array([[[ 1.68678801e+04+1899.59541572j]],

       [[ 4.88149630e+03+5695.62368911j]],

       [[-1.65223253e+03+1446.65857603j]],

       [[-2.86299374e+02-1023.54967391j]],

       [[ 2.03202825e+02 +266.61931044j]],

       [[-9.01421678e+00   -8.59455602j]],

       [[-7.60915981e+01  +70.32174459j]],

       [[-3.23831146e+00  -15.10352513j]],

       [[ 9.29719328e+00  -14.52380567j]],

       [[ 1.52972108e+01  -15.75509395j]]])
Coordinates:
    g              float64 8B 9.81
    rho            float64 8B 1.025e+03
    body_name      <U16 64B 'WaveBot_immersed'
    water_depth    float64 8B inf
    forward_speed  float64 8B 0.0
  * wave_direction (wave_direction) float64 8B 0.0
  * omega          (omega) float64 80B 1.885 3.77 5.655 ... 15.08 16.96 18.85
  * influenced_dof (influenced_dof) <U5 20B 'Heave'
    period         (omega) float64 80B 3.333 1.667 1.111 ... 0.3704 0.3333
```

Figure 2.18: xarray Data Structure

As can be seen from the optimization problem it is a constrained one. Dynamical equations can be passed into an optimization problem as an equality constraint. Solving a constrained optimization problem where an equality constraint ($r(x) = 0$) is used to enforce the dynamics of the system and inequality constraints used to regulate the operation limits of the WEC system.

The dynamics of the linear WEC system can be represented with the residual form of cummins' equation as shown in eq. 2.33.

$$r = -(M + m_a)\ddot{x} - Kx - B\dot{x} - C\int_{-\infty}^{t} \dot{x}(\tau)\, d\tau + F_{\text{ext}} + F_{\text{exc}} = 0 \tag{2.33}$$

Here, x includes both the states of body motion, denoted by x_{pos}, and other external states, x_{ext} (e.g., those associated with controllers, PTO systems, mooring systems, etc.). The dimension of the states shown in eq. 2.34.

$$x_{\text{pos}} \in \mathbb{R}^m(2n+1), \quad x_{\text{ext}} \in \mathbb{R}^p(2n+1) \tag{2.34}$$

Where m is the number of body modes of motion, n is the number of frequency components, p is the number of external states.

To discretize the control problem by using pseudo-spectral method, it is needed to approximate the position, velocity, and force vectors with a linear combination of the basis functions. In Wecopttool, fourier series are used as basis functions. To understand how WecOptTool employs this theory, some methods will be reviewed.

For example, `time_matrix()` method is used for calculating the time domain of a signal from its frequency coefficients. Time domain x(t) is calculated by Mx, where M is the time matrix. Similarly, the state of its derivative can be calculated with Dx, where D is the derivative matrix. In the library it is defined as `derivative_mat()`. You can also find the double derivative method `derivative2_mat()` in the library.

After the discretization of the dynamical equations, the forces are converted to a residual form ($r = ma - \Sigma f$). To be used in the optimization problem as a constraint. It is done by the `residual()` method, which is included in the solve() method.

Objective function is created with the help of `time_mat()` and `derive_mat()` methods. They are used for calculating the pto force and velocity (derivative of position) in the time domain.

The optimization problem is solved by using the Sequential Least Squares Programming optimizer from the Scipy library in the solve() method.

In conclusion, non-parametric complex impedance data is required, which can be obtained from WECSim. Additionally, wave excitation force coefficients are necessary. These complex coefficients can be calculated using data from WECSim, specifically through an estimation process.

Chapter 3

Methodology

The steps followed in this project are thoroughly outlined in this chapter, which is divided into separate sections that cover key elements of the framework and how it was put into practice.

The chapter starts with **Framework**, where the general scheme and folder structure of the framework are provided, and continues with **Model Selection**, where a model is selected to demonstrate the methodology. In the **Identification** section, the focus is on determining the impedance data that employ the dynamics of the selected model. Section **Estimation of Excitation Forces** shows the process used to obtain and calculate the excitation forces of waves acting on the WEC. The method also includes selection of the cutoff frequency at which these forces become less important by comparing the wave spectrum and impedance data. Fourier coefficients were filtered to reduce calculation errors at this stage. **Optimization** shows the application of the pseudo-spectral method within WecOptTool to improve energy harvesting performance while respecting operational constraints. In the **Runtime Minimization**, the focus is on improving computing efficiency. By delving into the problem formulation of the pseudo-spectral method, the steps required to minimize the computation time are described. Finally, the section **Extensions to the Framework** discusses how the proposed methodology can be scaled to multiple DoFs. Each of these sections contains a detailed description of the relevant tasks, thereby creating a consistent methodology that supports the goals of the project.

3.1 Framework

This section outlines the framework and its key components, which are organized into folders and files for modularity and streamlined execution.

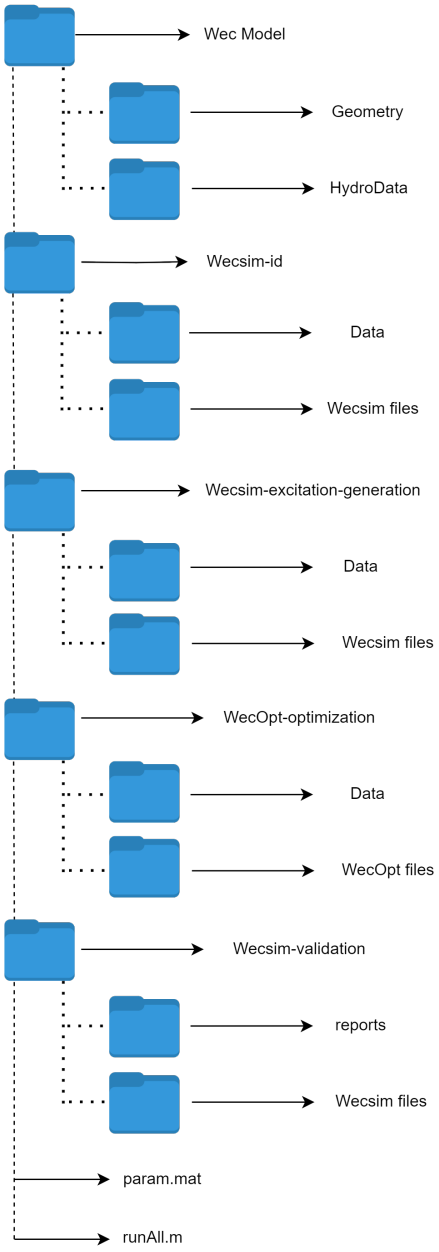

Figure 3.1: Folder Structure Diagram of Framework

WEC Model consists of two main folders: *Geometry* (containing STL files) and *Hydrodata* (containing H5 files). The H5 file can be generated by running the `bemio` code.

Wecsim-id consists of two folders. The identification process was performed using the files in *Wecsim Files* folder. The impedance data generated at the end of the WECSim simulation is kept in the *Data* folder.

Wecsim-excitation-generation is responsible for wave elevation generation and excitation force estimation. The *Wecsim Files* folder has the simulation files, and the *Data* folder stores the Fourier coefficients of the estimated excitation force and modified impedance data from the simulations.

WecOpt-optimization has two folders. In the *WecOpt Files* folder, a constrained optimization process was performed to obtain the optimal PTO force according to the impedance and excitation force coefficients that were saved in the previous steps. The optimization results, such as the PTO force, position, velocity, etc., are saved into the *Data* folder.

Wecsim-validation is where the validation of WecOptTool results occurs. Using the optimal PTO force from the previous step, the responses of WECSim and wecopttool were compared. It's an extra step just used for validation.

Finally, the `runAll.m` script automates the simulation process by sequentially executing the workflows of each folder. When the model is changed, it is essential to review each folder to ensure accurate results and proper configuration. This modular framework ensures flexibility and reliability to achieve project objectives.

3.2 Model Selection

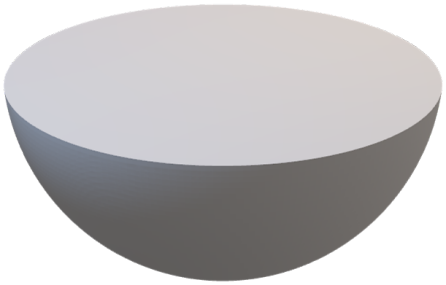

Figure 3.2: Sphere Model

To demonstrate the framework and the development of the methodology, a single-degree-of-freedom (DoF) single-body device (a sphere) was used, as shown in fig. 3.2. This design was motivated by the simplicity of its hydrodynamic

data and its suitability for understanding the fundamentals of both WECSim and WecOptTool. Because it has a simple structure, unnecessary complications such as multi-DoF control are avoided, and the focus is on energy extraction from the heave motion of the device. By simplifying the problem, the framework development and methodology validation were straightforward and efficient.

The key parameters of the sphere model are shown in table 3.1.

Body	**Mass (tonne)**	**Direction**	**CoG (m)**	**Inertia Tensor (kg m^2)**
Sphere	261.724	x	0	20,907,301
		y	0	21,306,090
		z	-2	37,085,481

Table 3.1: Properties of Sphere Model

3.3 Identification

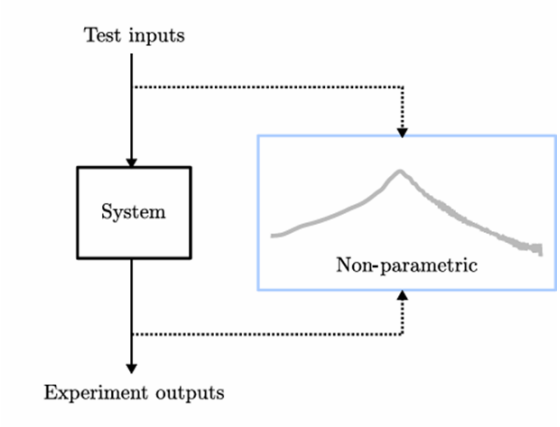

Figure 3.3: Non-parametric Identification

The dynamics of the WEC must be identified correctly because this data are used to introduce the WEC during the optimization stage. In the case of WecOptTool, wave excitation force coefficients and WEC impedance are required. Given the numerous options for defining a WEC object in the optimization tool, a straightforward and generalizable approach was chosen for this study.

The identification stage for the WEC dynamics was carried out without parameterization (fig. 3.3)to simplify the framework and enhance generalizability.

This approach enables the determination of the relevant impedances between the control axis and the WEC axis without the need to compute specific parameters or account for the order of the differential equations. Since WecOptTool operates solely in the frequency domain and computes the steady-state response, providing Fourier coefficients of the impedance data is more than sufficient.

To deal with the discrepancies between the transient and steady-state solutions, the simulation time was set to 100 s, yielding a fundamental frequency resolution of 1e-2 Hz. This resolution is sufficient to accurately capture the device response across the device operation range.

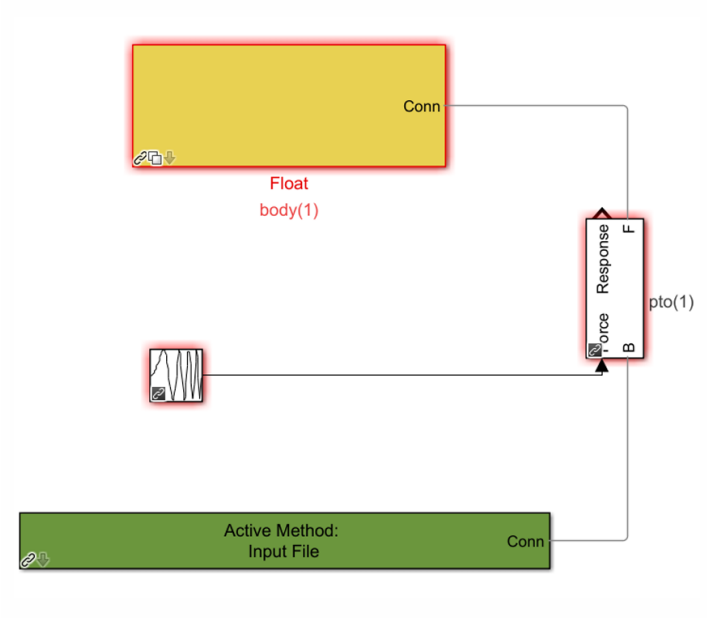

Figure 3.4: Chirp Signal acting as actuation

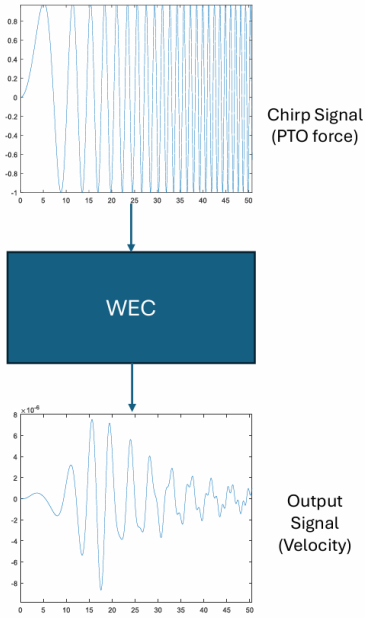

Figure 3.5: Identification process

A chirp signal is employed as an identification method to stimulate the system across a range of low to high frequencies, thereby accurately capturing its dynamics. WECSim is an effective tool for straightforward implementation of this type of application. To implement the actuation force as a chirp up signal, 'translational actuation' block is used to incorporate the actuating force. This block can also output the force response to be used in closed-loop control systems. The proposed method is implemented in fig. 3.4 and fig. 3.5.

The Fourier transforms of the applied chirp signal force and body velocity response were computed in Matlab. By considering zero elevation input, no additional forces were applied to the body during the simulations. Similar to

electrical engineering, the impedance data represent the effort divided by the flow variable. The force exerted on the wec body in relation to the device's velocity is equivalent to the voltage over the current in electrical engineering.

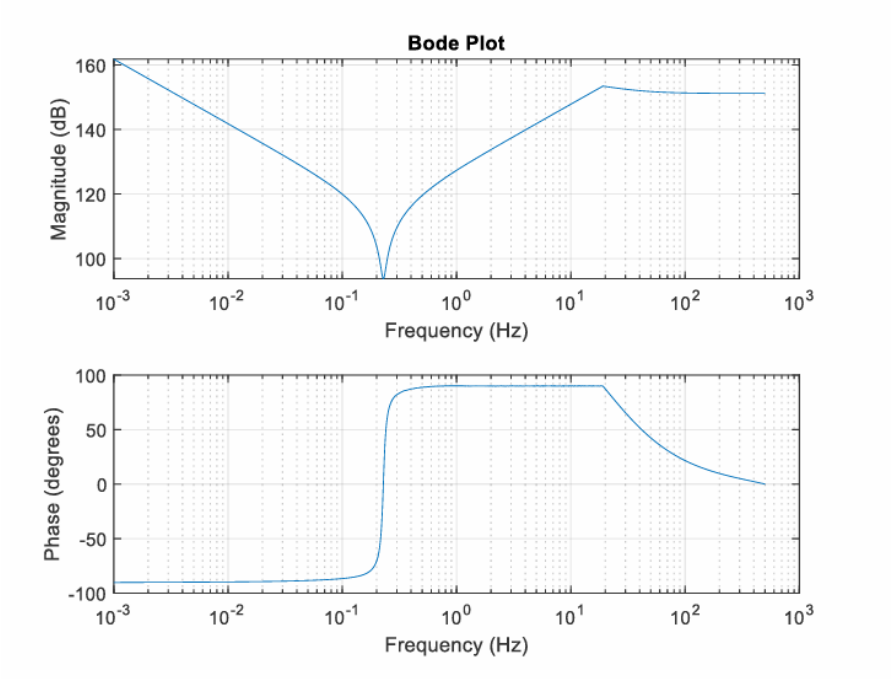

Figure 3.6: Identified Impedance

The non-parametric representation of the WEC impedance can be found using the following formula:

$$I(jw) = Fpto(jw)/V(jw) \tag{3.1}$$

where F_{pto} and V are the complex coefficients of the PTO force and velocity. The identified impedance for the sphere model is shown in fig. 3.6.

3.4 Estimation of Excitation Forces

The working principle of the WEC device is illustrated in the block diagram in fig. 3.7. As can be seen, the WEC device can be, in general, a multiple-input system. One of the inputs is the wave excitation force, which is induced by waves in the ocean and depends on some dynamics because of the body shape and properties. The transfer function G_{exc} coincides with these dynamics and converts the wave elevation to the force applied to the body. To simplify the optimization process and cancel another complexity element, it is necessary to eliminate the wave elevation and thus to identify the wave excitation directly. This way, we do not have to think

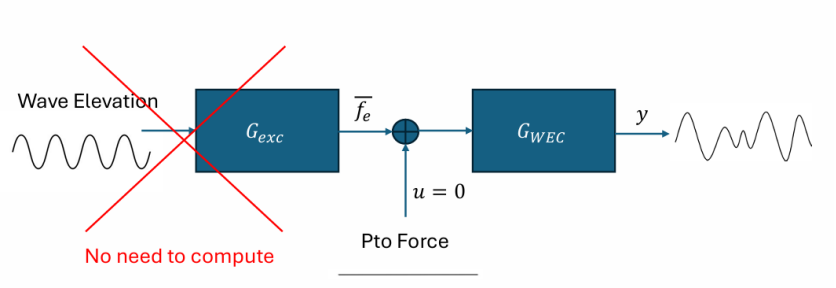

Figure 3.7: Estimation of Wave Excitation Force

about storing and supplying the same wave elevation to the optimization tool. It is as generalized and simplified as possible.

This process includes modifying the impedance data by selecting a cut-off frequency, estimating the Fourier coefficients of the wave excitation force, and filtering out unwanted errors. This process is explained in the following subsections.

3.4.1 Choosing cut-off frequency

Choosing cut-off frequency is an important step to decrease the time needed to finish the calculations carried out in Matlab and the running time of optimization. By choosing a cutoff frequency, the insignificant frequencies are eliminated. The application of choosing this frequency is explained in detail in the following paragraph.

First, the impedance data are normalized, and the frequency index at which the magnitude falls below -20 dB is identified. Similarly, the wave elevation spectrum is analyzed by normalizing the incoming wave data to detect any higher-frequency components with relatively significant amplitudes. The corresponding frequency index is then determined for the wave spectrum. The final step in selecting the cutoff frequency involves comparing the indices derived from the normalized impedance data and the wave spectrum. The higher frequency value was selected to ensure that the device response was captured accurately. This approach accounts for all significant dynamics and ensures that the system is modeled correctly. The procedure is described in Algorithm 1 and presented in fig. 3.8.

Algorithm 1 Impedance Cutoff Algorithm

```
procedure ImpedanceCutoff(impedance_data, wave_spectrum, threshold)
    ▷ Normalize impedance data
    norm_impedance ← Normalize(impedance_data)
    ▷ Normalize wave spectrum data
    norm_spectrum ← Normalize(wave_spectrum)
    ▷ Set threshold for cutoff
    magnitude_threshold ← threshold
    ▷ Find points near the threshold value
    threshold_points ← FindPointsNearThreshold(args)
    ▷ Locate maximum value within threshold points
    max_value ← max(threshold_points)
    ▷ Identify pre- and post-cutoff indices
    pre_index, post_index ← FindIndices(norm_impedance, max_value)
    return pre_index, post_index
    ▷ Return cutoff indices
end procedure
```

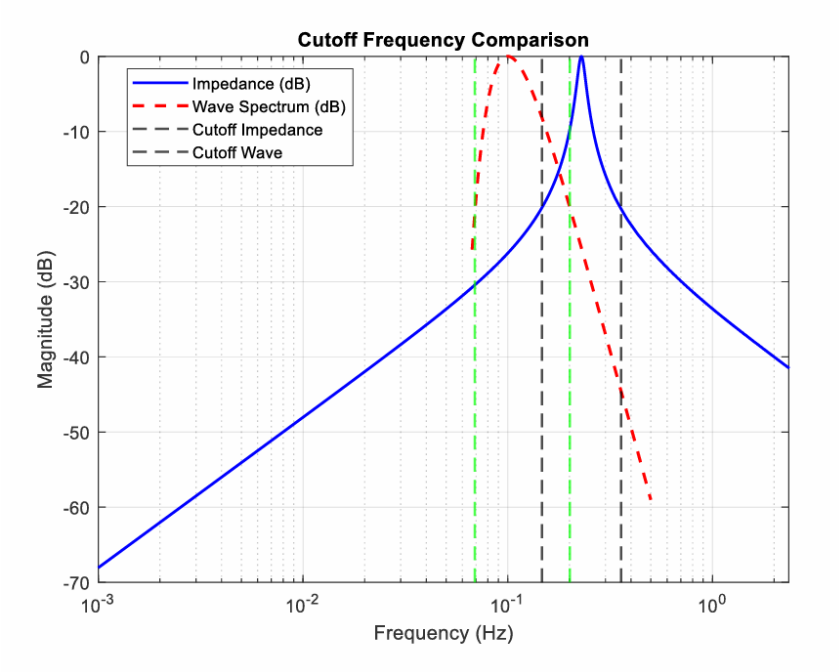

Figure 3.8: Comparison of Cut-off Frequencies

3.4.2 Estimation Process

To incorporate the wave excitation force, it is essential to estimate its Fourier coefficients. After taking the velocity of the DoF where the PTO force is applied, it is needed to find the length of each realization, remove the mean, and calculate the frequencies for the FFT. The frequency interval is the same as the impedance data. The next step was to import the impedance frequency and magnitude arrays. The estimated excitation force was calculated by multiplying the impedance data by the FFT of the device velocity as shown in eq. 3.2.

$$F_{exc}(jw) = V(jw)I(jw) \tag{3.2}$$

3.4.3 Filtering

Waves generated by winds have periods 1-20 s and period with highest energy scale is around 8 s.[27]. In the thesis the wave periods between 3-15 s are utilized. This translates to frequencies in the range:

$$f = \frac{1}{15} - \frac{1}{3} = 0.0667\,\text{Hz} - 0.3333\,\text{Hz} \tag{3.3}$$

A Butterworth Bandpass filter can be designed that can only allow the signal to pass in this frequency range with the following equation:

$$[b, a] = \text{butter}(n, [w_l, w_h],' bandpass') \tag{3.4}$$

where n is the filter order, w_l being the lower limit, and w_h being the upper limit.

The lower and upper frequency limits constrained between 0 and 1 Hz in the `butter` function. For our application, the fundamental frequency is 1×10^{-2} Hz. The values of the filter are sampled using `freqz`(b, a, n, fs) and applied to the estimated excitation data. Here, $fs/2 = 1$ is nyquist frequency, $fs/2N = f_0$ is fundamental frequency and $n = \frac{1}{f_0}$.

In fig. 3.9, the application of the filter is shown. The original signal has some unwanted elements in the first harmonics, and the sampled filter successfully filters it and keeps the information in the middle range.

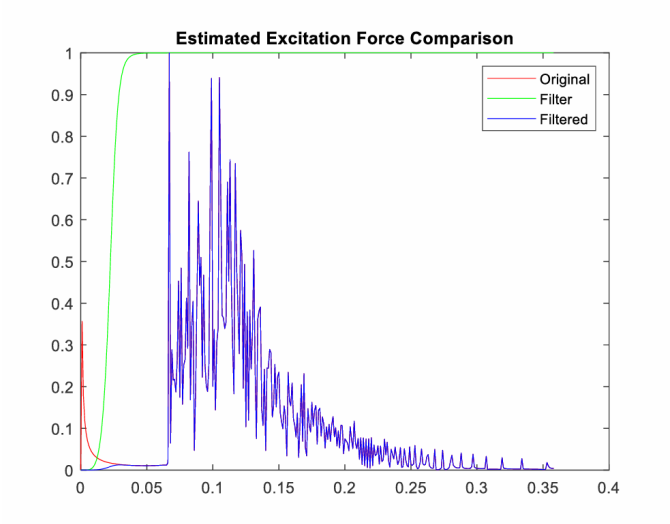

Figure 3.9: Filter Comparison

3.5 Optimization

After calculating the wave excitation force coefficients, these values must be integrated into WecOptTool. To bypass the requirement for defining a wave elevation which is used for the excitation force calculation in WecOptTool, a workaround method is employed. The magnitude of the wave elevation is set to unity across the entire frequency range. This approach ensures that the estimated force can be used directly, eliminating the dependency on a wave elevation definition while maintaining compatibility with the tool. The updated workflow is shown in fig. 3.10.

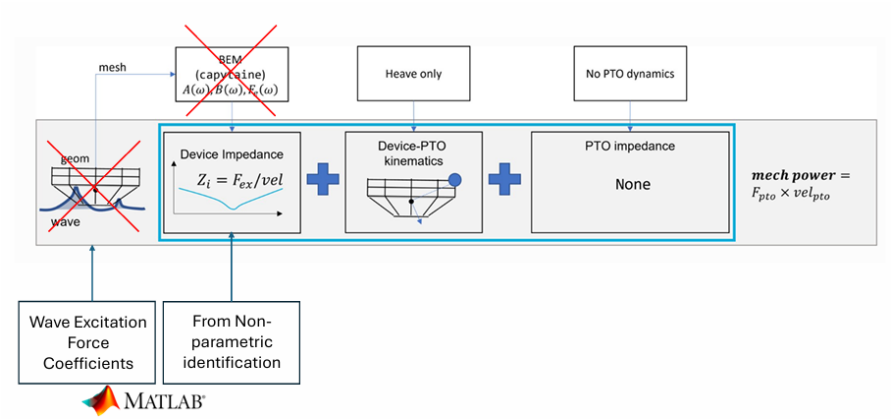

Figure 3.10: Updated Workflow for Optimization

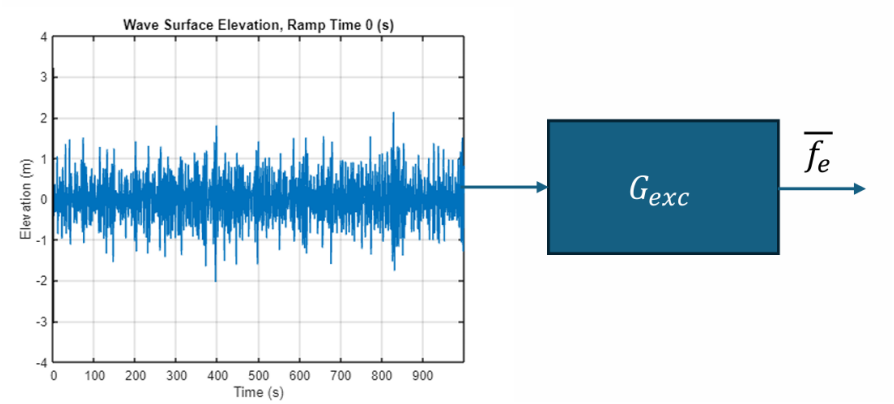

Figure 3.11: Wave Elevation as Input

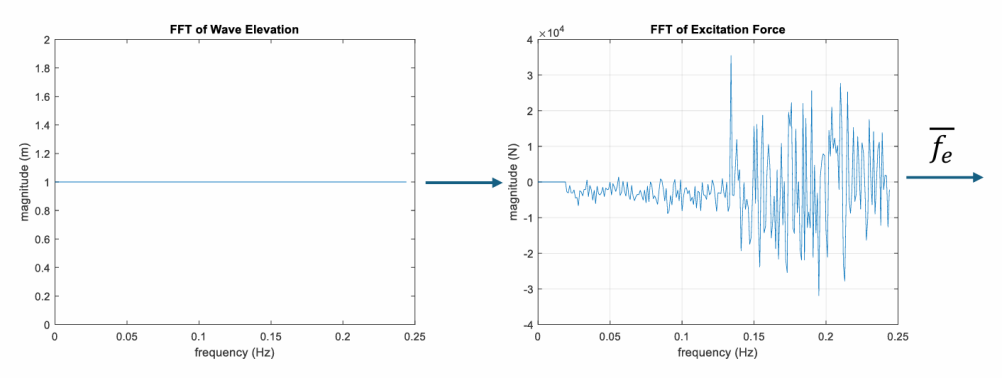

Figure 3.12: Workaround Method

The usage of wave elevation in WecOptTool and the employed method are shown in fig. 3.11 and fig. 3.12, respectively.

Another important aspect of the optimization is introducing the non-parametric device impedance. It is important to choose the same number of harmonics in order to avoid errors and choosing the correct frequency points for the accuracy of the results. Then the remaining step is enforcing constraints. The constraints can be special functions and derived according to the user's needs. There can be constraints on the position, velocity, acceleration of the device, and pto force. To keep the simplicity of the application, no PTO dynamics are assumed. As the objective function, mechanical power maximization is considered.

3.6 Runtime Minimization

The objective function of the optimization is stated with the eq. 3.5. As it can be noticed, it is quadratically proportional to the PTO force. This objective function has a size of N, which affects the duration of the optimization process greatly [21].

$$J^N = -\frac{T}{2}\hat{\boldsymbol{u}}^\top \boldsymbol{G}^{-1}\hat{\boldsymbol{u}} - \frac{T}{2}\hat{\boldsymbol{u}}^\top \boldsymbol{G}^{-1}\hat{\boldsymbol{e}} \tag{3.5}$$

Constraints provided for the optimization, such as equality and inequality, can be seen in the following equation. In our case, inequality constraints for maximum allowed pto force and stroke distance are used. It can be noticed that the number of time instants for the constraints is Nc. When N is different than Nc, it means that inequality constraints are only applied to a set of equally intervalized points to facilitate the optimization process.

$$\begin{aligned} \Phi\left(t_k\right)\hat{\boldsymbol{u}} \leq F_{\max}, \quad -\Phi\left(t_k\right)\hat{\boldsymbol{u}} \leq F_{\max} \\ \Phi\left(t_k\right)\hat{\boldsymbol{x}}_1 \leq Z_{\max}, \quad -\Phi\left(t_k\right)\hat{\boldsymbol{x}}_1 \leq Z_{\max} k = 0, \ldots, N_c \end{aligned} \tag{3.6}$$

In summary, the computational load depends on N (the number of harmonics) and N_c (the number of constraints), making the choice of N and w_0 (fundamental frequency) critical. A smaller provides finer frequency resolution but increases N over the same frequency range, leading to a larger NLP (nonlinear programming) problem.

To reduce the computational load, the largest frequency component with significant energy content is identified, and higher frequency components beyond this point are discarded. By selecting this cut-off frequency, the resolution of the impedance data can be adjusted to retain sufficient information about the system dynamics while minimizing N and optimizing computational efficiency.

3.7 Extensions to the Framework

In this section, the extensions for the scaling of the Framework for Multi-DoF capabilities will be reviewed. Until now, the control is only applied in a single DoF. Pseudo-spectral method can tackle the optimization task with multiple DoF impedance data but in order to do it the structure of the code should be modified. For the brevity of the thesis, this work left for the future projects but some context and methodology will be mentioned in this section.

3.7.1 Generalized Excitation Force Estimation

The excitation and system behavior are represented using the matrix formulation show in eq. 3.7 [24].

$$V_u = \begin{bmatrix} G_u & G_{\bar{u}} \end{bmatrix} \begin{bmatrix} F_u - U \\ F_{\bar{u}} \end{bmatrix} \tag{3.7}$$

Here, $G_u \in \mathbb{C}^{m \times m}$ is the dynamic mapping of the m controlled DoFs, and $G_{\bar{u}} \in \mathbb{C}^{m \times (N-m)}$ represents the dynamic mapping of the $(N-m)$ uncontrolled DoFs. $V_u \in \mathbb{C}^m$ is the velocity matrix containing the velocities of the m controlled DoFs. $F_u \in \mathbb{C}^m$ and $F_{\bar{u}} \in \mathbb{C}^{(N-m)}$ are the excitation forces acting on the m controlled and $(N-m)$ uncontrolled DoFs, respectively. $U \in \mathbb{C}^{(N-m)}$ is the control input applied to the $(N-m)$ uncontrolled DoFs.

Since only the controllable DoFs can be actuated to maximize the energy absorption, there is no need to estimate the uncontrolled dynamics. With this way, the excitation force $\tilde{F}_u$ can be estimated with the eq. 3.8.

$$V_u = G_u \left[\tilde{F}_u - U \right] \tag{3.8}$$

Current Implementation

For the sphere, the system is under-actuated, with a single DoF Power Take-Off (PTO). Scaling is unnecessary unless two or more control DoFs are introduced. For the current single-DoF implementation:

- $F_{\text{pto}}/V_{\text{pto}}$ is identified, which suffices for the optimization.
- The excitation coefficient array $F = IV$ is straightforward to compute since only one DoF is considered.

Extended Implementation

If additional DoFs are introduced, scaling is straightforward:

$$F_{\text{est}} = G_u^{-1} V \tag{3.9}$$

where G_u corresponds to the coupled impedance matrix for each additional DoF.

As an example let's think of an impedance length of 42 and 3 contol DoFs. The matrix sizes should be in the following configuration:

- **Impedance**: $3 \times 3 \times 42$
- **Velocity**: $3 \times 3 \times 42$
- **Estimated Excitation Force**: $3 \times 3 \times 42$

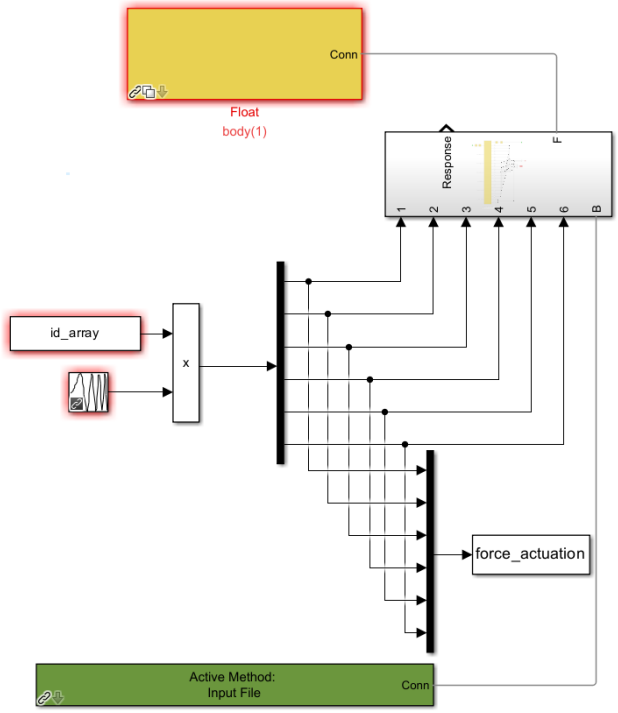

Figure 3.13: Multiple-Dof Identification

In fig. 3.13, a floating (6 DoF) PTO block is modified for the application of actuation force to carry out the identification process in multiple axes. The chosen control DoFs from the example can be introduced to the WECSim as an array and the impedance can be calculated in a for loop.

Chapter 4

Simulation and Results

In this chapter, the results of the conducted simulations will be shared. Two different models are chosen for the key study to do a comparative analysis and show the strength of the framework to deal with different configurations. As explained in the methodology section, all the necessary data that needs to be collected will be shown in this chapter and will be compared in the same plots to show the differences between the devices. Constrained simulations will be carried out, and as a result, the power matrices will be presented for the overall conclusion.

In the **Models** section, the models are selected for the simulation, and related data are presented for these models. **Validation: WECSim vs. WecOptTool** presents the data used to validate the coupling between WECSim and WecOptTool. It compares optimization results under identical wave elevations, demonstrating the consistency and reliability of the integrated frameworks. In the **Constrained Optimizations** section, the results of the PTO distance-constrained optimization for the RM3 and the torque-constrained optimization for the OSWEC are presented. **Power Matrices** section presents the scatter matrices for both devices, allowing the performance evaluation in different sea conditions.

4.1 Models

4.1.1 RM3

As the first model, the RM3 (Reference Model 3) two-body point absorber is chosen, and the 3D model with the dimensions is shown in fig. 4.1. The model is present in the WECSim applications repository as an example of geometry. The parameters are imported from the existing dataset in WECSim. The device consists of two bodies, which are named float and plate. It is chosen to show the effectiveness of

the framework while dealing with multi-body systems.

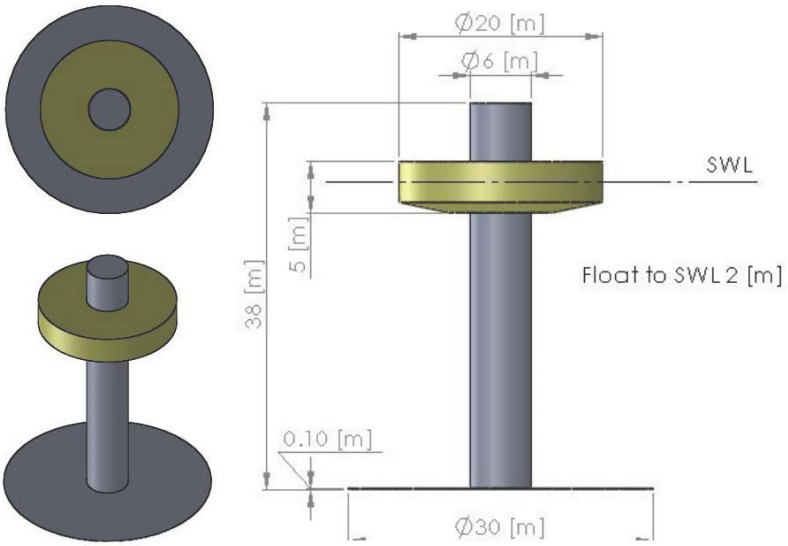

Figure 4.1: RM3

The properties of the RM3 model are shown in table 4.1.

Body	Mass (tonne)	Direction	CoG (m)	Inertia Tensor (kg m^2)
Float	727.01	x	0	20,907,301
		y	0	21,306,091
		z	-0.72	37,085,481
Plate	878.30	x	0	94,419,615
		y	0	94,407,091
		z	-21.29	28,542,225

Table 4.1: Mass, Center of Gravity, and Inertia Tensor for Each Body

The RM3 Simulink model is shown in fig. 4.2. It is represented with two floating bodies. The constraint block is used to limit the motion in specific degrees of freedom. The PTO block is used for the actuation of the PTO placed between the two bodies. The optimal PTO force is calculated according to the relative motion of the bodies in the optimization tool.

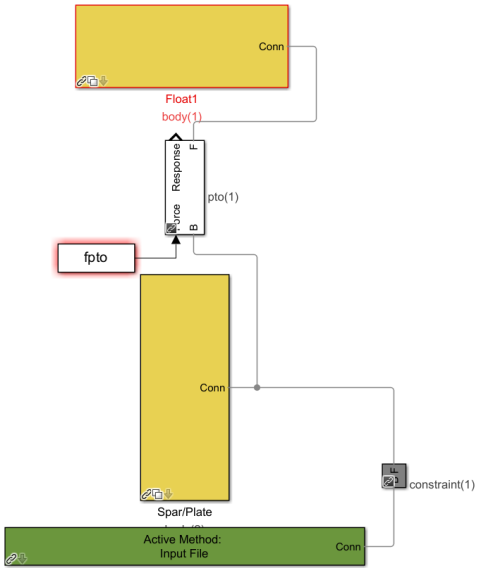

Figure 4.2: RM3 Simulink Representation

4.1.2 OSWEC

As the second model, the OSWEC (oscillating surge wave energy converter) is selected. Its 3D model with the dimensions is shown in fig. 4.3. This model exists in the WECSim applications repository. The solution of the boundary element method for this model is solved using the BEMIO code and used in the simulations as the dataset. This device consists of two bodies. One of the bodies is used to fix the device to the sea bottom and doesn't affect the dynamics significantly. The other part is the moving part, which is called the flap. As the name of the device suggests, the flap acts in the surge (pitch). This device is selected to show the capability of the framework in other control DoFs.

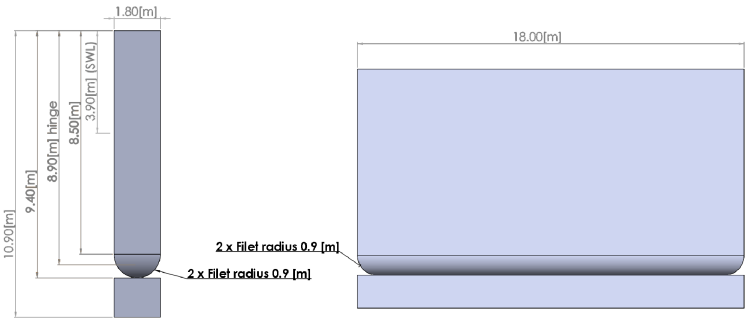

Figure 4.3: OSWEC

The properties of the OSWEC model are shown in table 4.2.

Body	Mass (tonne)	Direction	CoG (m)	Inertia Tensor (kg m^2)
Flap	127	x y z	0 0 -3.9	0 1,850,000 0

Table 4.2: Mass, Center of Gravity, and Inertia Tensor for Flap

The Simulink model of OSWEC is shown in fig. 4.4. It represented with two floating bodies. The constraint block is defined for the device, and the rotational PTO is defined for the actuation in the surge motion.

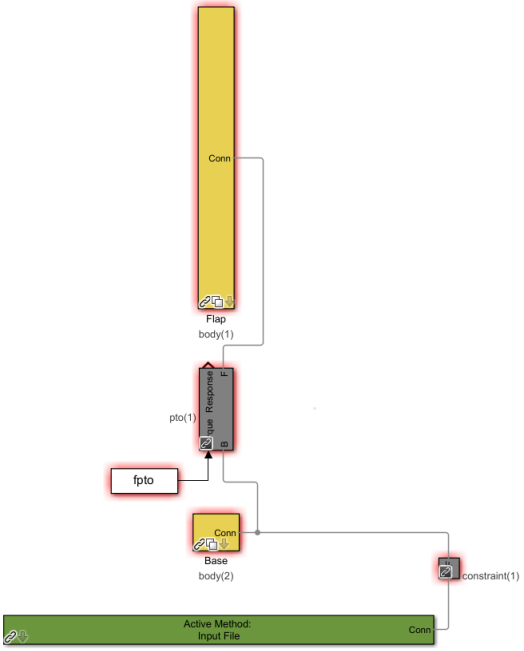

Figure 4.4: OSWEC Simulink Representation

4.2 Validation: WECSim vs. WecOptTool

4.2.1 Wave Elevation

The wave elevation is generated using the Pierson-Moskowitz spectrum with a height of 8 m and a period of 12 s. In fig. 4.5, the wave elevation used for the simulations carried out in this section is presented.

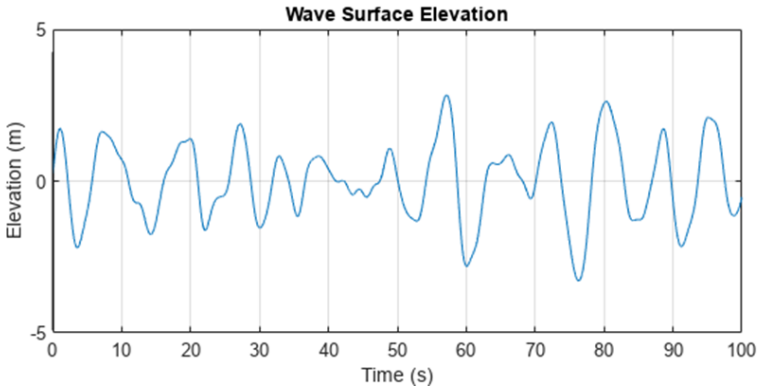

Figure 4.5: Wave Surface Elevation

4.2.2 Identified Impedance

Fig. 4.6 presents the impedance data for both devices. In the RM3's case, the inverse of its impedance has two peaks, and this is caused because it consists of two floating bodies, and those are designed to have different resonance frequencies to create a relative motion with the incoming waves. This behavior is absent in the OSWEC, as its only moving component is the surging flap.

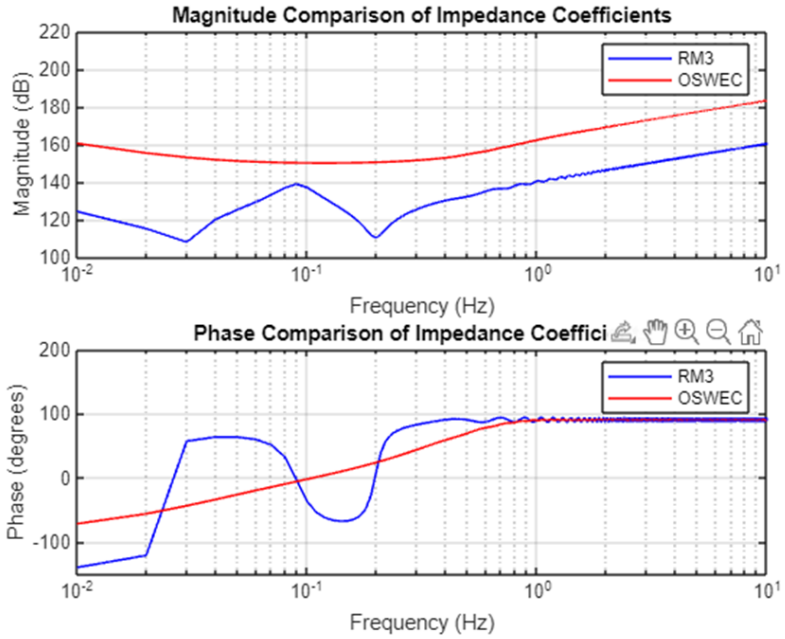

Figure 4.6: Comparison of Impedances

Another interesting result is that the impedance of the OSWEC is higher than that of the RM3's across all the operational frequency ranges. This means that the torque-to angular speed ratio of OSWEC is higher than the force-to-linear speed ratio of RM3. Since the two devices have different control DoFs, the results should be carefully reviewed.

4.2.3 Estimated Excitation Coefficients

In fig. 4.7, estimated excitation coefficients acting on the RM3 and OSWEC are shown. These excitation coefficients are directly related to the device's body shape and the wave elevation. For the different wave elevations, the values will be different. It is evident that the excitation acting on the devices is force for RM3 and torque for OSWEC.

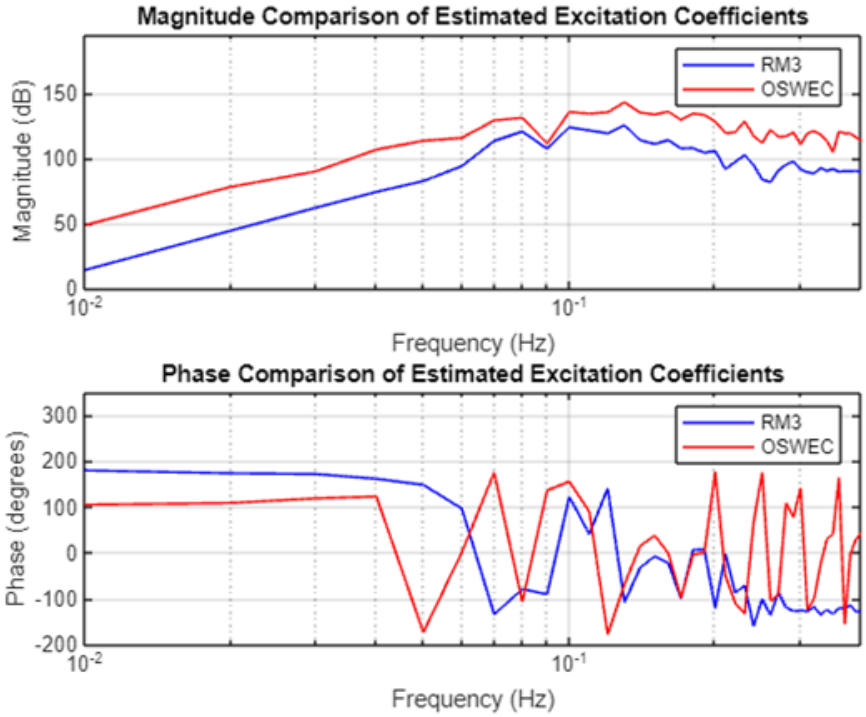

Figure 4.7: Comparison of Excitation Coefficients

4.2.4 Comparison for RM3

An optimization for PTO force limit of 1000 N is carried out, and the resultant optimal force is used in WECSim to compare the responses of WECSim and WecOptTool.

Fig. 4.8 shows the velocity response of RM3. The matching results confirm the accuracy of the optimization data.

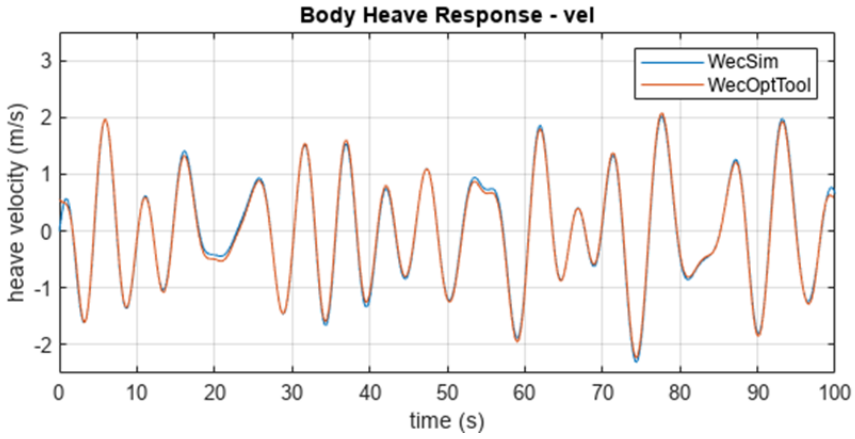

Figure 4.8: Heave velocity response of RM3

In fig. 4.9, the optimal PTO force is shown.

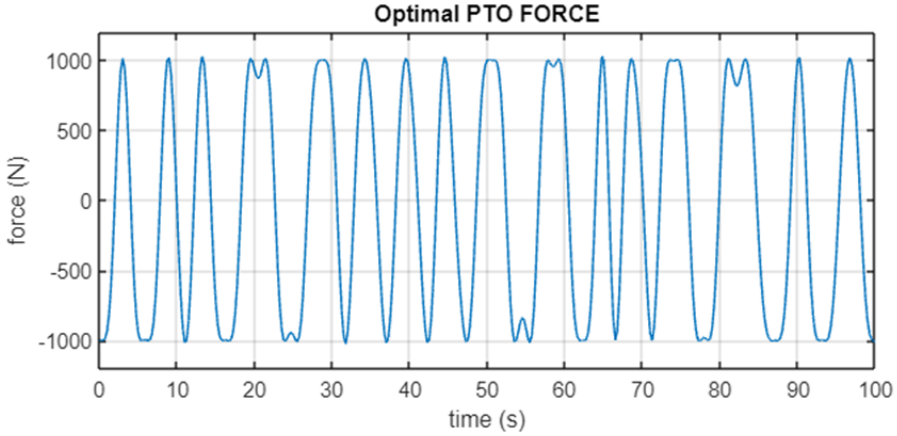

Figure 4.9: Optimal PTO Force for RM3

In fig. 4.10, the calculated mechanical power from WECSim and WECOPTOOL is shown. Again, the results are matching and showing the efficiency of the framework.

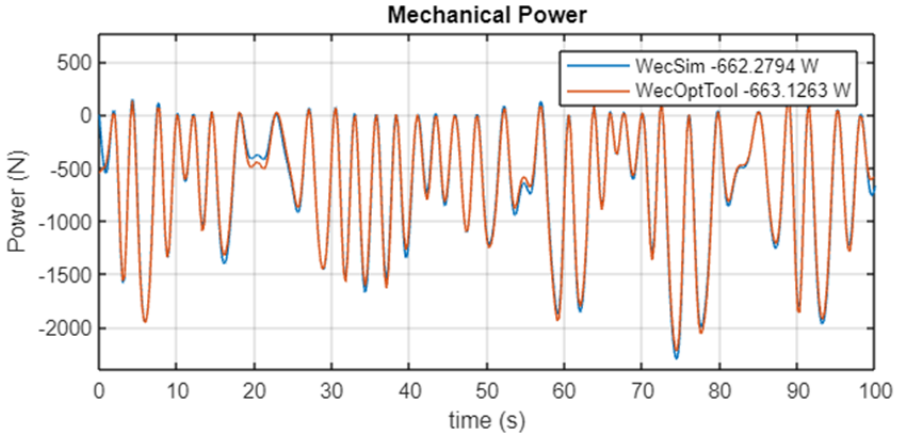

Figure 4.10: Extracted power from RM3

4.2.5 Comparison for OSWEC

For the analysis of OSWEC, a 1000 N of PTO force is used as a limit in the optimization tool.

Fig. 4.11 illustrates the velocity response of OSWEC, demonstrating identical behavior in both simulations.

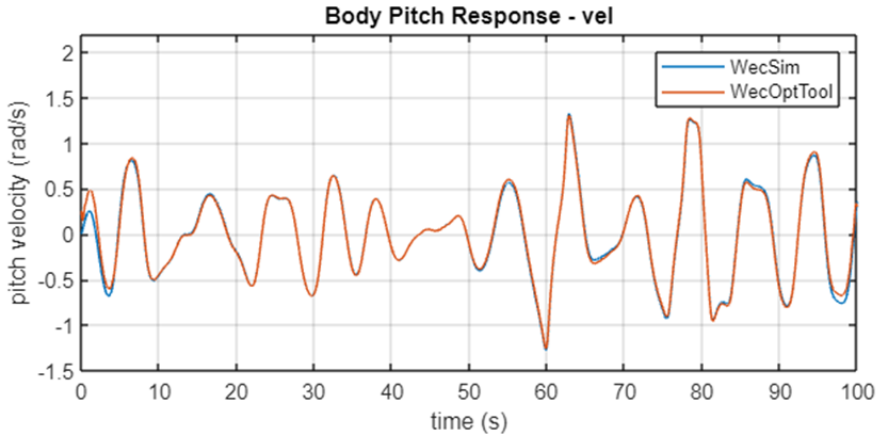

Figure 4.11: Pitch Velocity Response of OSWEC

In fig. 4.12, the optimal pto torque is shown.

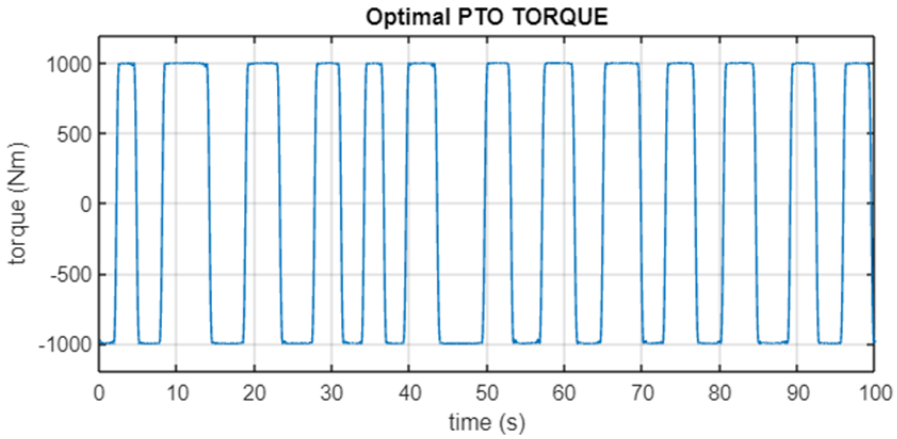

Figure 4.12: Optimal PTO Torque for OSWEC

In figure 4.13, the calculated mechanical power from WECSim and Wecopttool is shown. Again, the results are matching and showing the efficiency of the framework.

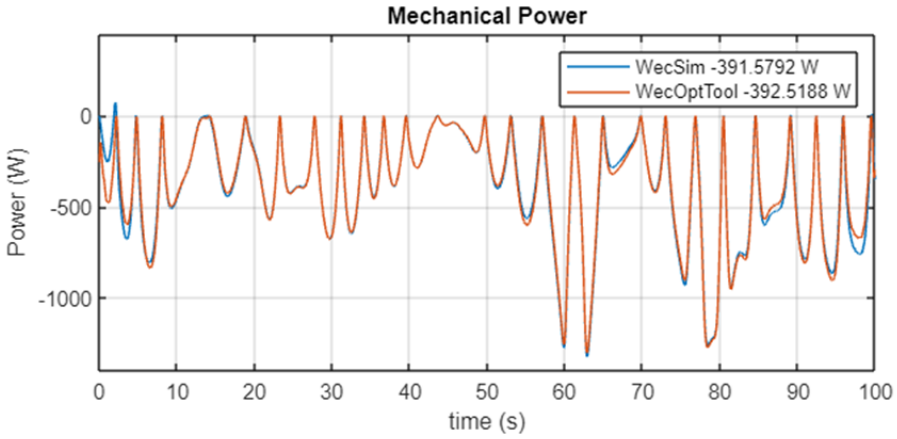

Figure 4.13: Extracted power from OSWEC

4.3 Constrained Optimizations

The constrained optimizations were performed under the same wave scenario, characterized by a Pierson-Moskowitz spectrum with a significant wave height of 3 meters and a wave period of 8 seconds.The PTO position constraint is demonstrated through its application on RM3, while the torque constraint is demonstrated with an application on OSWEC.

4.3.1 Constrained Optimization for PTO Distance

Three PTO distance limits are chosen as 0.8 m, 1.2 m, 2 m. A sufficiently high force limit is selected to impose motion constraints on RM3.

Fig. 4.14 presents the position response of the RM3 for the optimization results under different constraints on PTO distance. The optimization adheres to the specified limits.

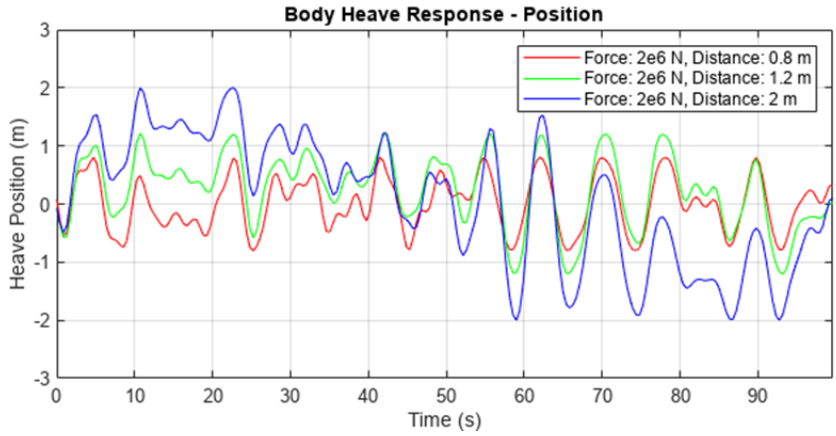

Figure 4.14: Position Response of RM3 for Various Distance Constraints

Fig. 4.15 presents the extracted power of the RM3 for the different constraints on PTO distance. For the constraints of 0.8 m, 1.2 m, 2 m, the average extracted powers are 7.37e4 W, 1.19e5 W and 1.6e5 W.

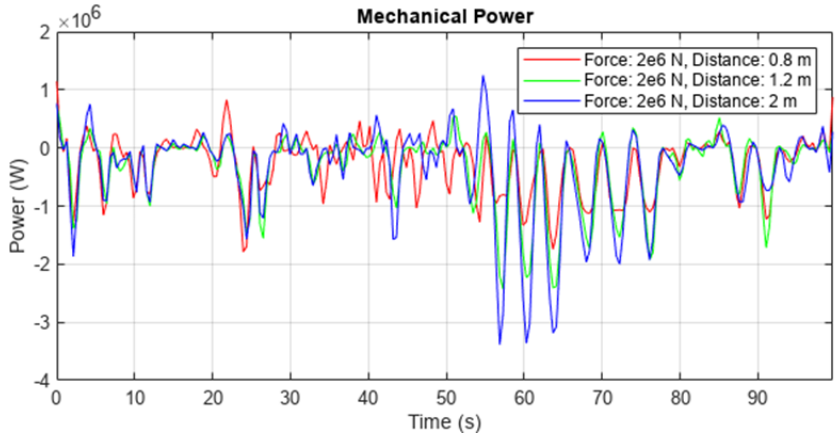

Figure 4.15: Extracted Power from RM3 for Various Distance Constraints

4.3.2 Constrained Optimization for PTO Torque

Three PTO torque limits are chosen as 0.5e6 N, 1e6 Nm, 2e6 Nm for the constrained optimization to show the effect of PTO torque on the power extraction. A high angle limit is selected to avoid overly restricting OSWEC's motion.

Fig. 4.16 presents the optimal forces of the OSWEC for the optimization results under different constraints of PTO torques. The optimization adheres to the specified limits.

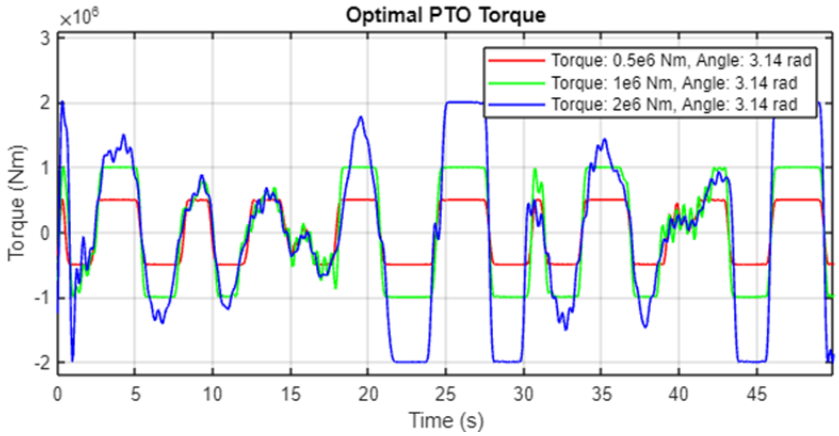

Figure 4.16: Optimal Torques of OSWEC for Various Torque Constraints

Fig. 4.17 presents the extracted power of the OSWEC for the different constraints on PTO torque. For the constraints of 0.5e6 Nm, 1e6 Nm and 2e6 Nm, the average extracted powers are 2.79e5 W, 3.39e5 W and 3.55e5 W.

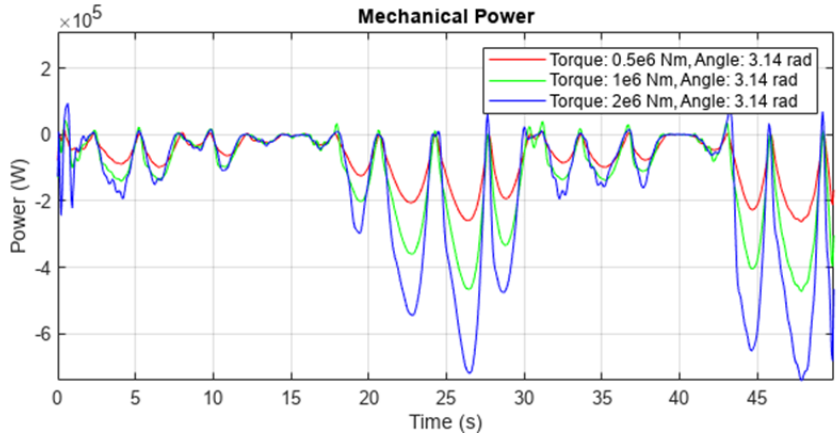

Figure 4.17: Extracted Power from OSWEC for Various Torque Constraints

4.4 Power Matrices

4.4.1 RM3

The power matrix of RM3 for a PTO which has a rating of 1e5 N force is shown in fig. 4.18.

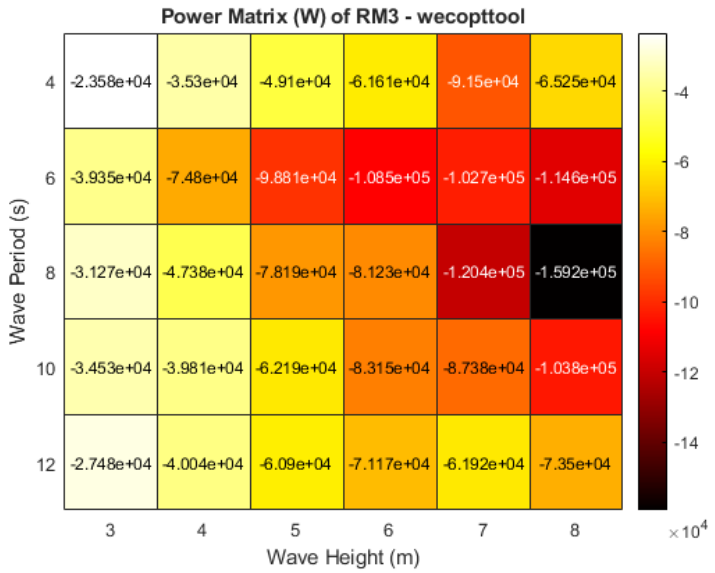

Figure 4.18: Power Matrix of RM3

The most significant captured energy happens at 8 m and 8 s.

4.4.2 OSWEC

The power matrix of OSWEC for a PTO which has a rating of 1e5 Nm torque is shown in fig. 4.19.

The most significant captured energy happens at 8 m and 8 s.

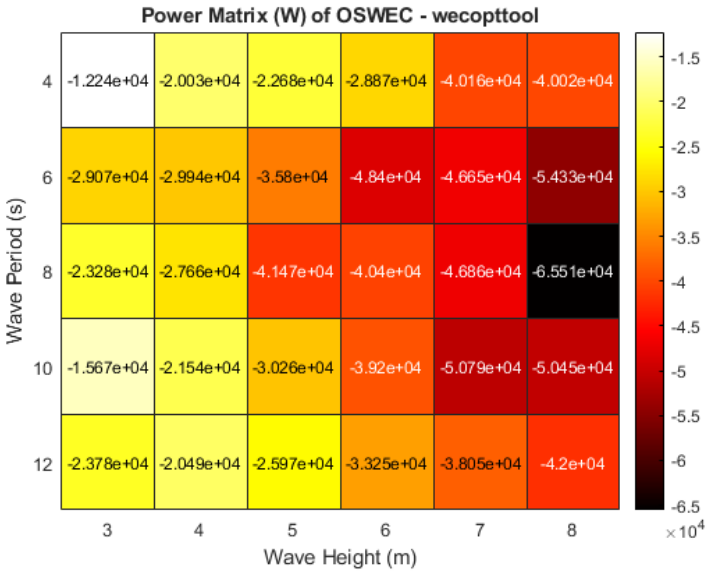

Figure 4.19: Power Matrix of OSWEC

4.4.3 Conclusion

The power matrices for both of the devices is generated using the framework. These matrices can be used in the performance evaluation of the devices in the different conditions and can help enhancing the model during the design process.

Chapter 5

Conclusion

5.1 Conclusion

This study presents a comprehensive framework for the analysis, identification, and optimization of WECs to simplify the energy maximization problem. It is done with one of the optimal control methods called the pseudo-spectral method, and the data used for the optimization is tailored using the data-based identification techniques and the estimation methods. Hydrodynamic simulation, system identification, and control optimization stages are integrated into this framework. The framework is tested and validated across different sea states, showing its effectiveness in capturing energy while adhering to constraints on PTO force and motion. Additionally, by using various configurations of the WECs, the study highlights the framework's flexibility and versatility. As a result, the power matrices of the OSWEC and RM3 devices are generated, providing valuable insights for their design and optimization processes.

5.2 Future Works

This framework lays a solid foundation for the further exploration and innovation of WEC technology. The future work would include the inclusion of nonlinearities in the analysis, scaling the framework to multiple-DoF control structures, adapting the framework for real-time applications, and integrating techno-economic assessment analysis into the framework. By addressing these future directions, the framework can evolve into a more powerful tool, helping to advance the field of wave energy and contribute to the transition towards renewable energy solutions.

Bibliography

[1] U.S. Energy Information Administration. *What is U.S. electricity generation by energy source?* 2024. URL: https://www.eia.gov/tools/faqs/faq.php?id=427&t=3 (visited on 02/29/2024) (cit. on p. 1).

[2] Frederica Perera and Kari Nadeau. «Climate Change, Fossil-Fuel Pollution, and Children's Health». In: *New England Journal of Medicine* 386.24 (2022), pp. 2303–2314. DOI: 10.1056/NEJMra2117706. eprint: https://www.nejm.org/doi/pdf/10.1056/NEJMra2117706. URL: https://www.nejm.org/doi/full/10.1056/NEJMra2117706 (cit. on p. 1).

[3] Joao Cruz. *Ocean wave energy: current status and future prespectives*. Springer Science & Business Media, 2007 (cit. on pp. 1, 2).

[4] International Renewable Energy Agency (IRENA). *Ocean Energy: Technologies, Patents, and Projects*. IRENA, 2020 (cit. on p. 1).

[5] Ronan Costello and Arthur Pecher. «Economics of WECs». In: *Handbook of Ocean Wave Energy* (2017), pp. 101–137 (cit. on p. 2).

[6] John Ringwood, Francesco Ferri, Kelley M Ruehl, Yi-Hsiang Yu, Ryan G Coe, Giorgio Bacelli, Jochem Weber, and Morten Kramer. «A competition for WEC control systems». In: *Proceedings of the 12th European Wave and Tidal Energy Conference 27th Aug-1st Sept 2017*. 831. European Wave and Tidal Energy Conference 2017. 2017, pp. 1–9 (cit. on p. 2).

[7] Bingyong Guo and John V Ringwood. «A review of wave energy technology from a research and commercial perspective». In: *IET Renewable Power Generation* 15.14 (2021), pp. 3065–3090 (cit. on p. 3).

[8] António F de O Falcão. «Wave energy utilization: A review of the technologies». In: *Renewable and sustainable energy reviews* 14.3 (2010), pp. 899–918 (cit. on pp. 6–10).

[9] Alessandro Toffoli and Elzbieta M Bitner-Gregersen. «Types of ocean surface waves, wave classification». In: *Encyclopedia of maritime and offshore engineering* (2017), pp. 1–8 (cit. on p. 6).

[10] Tunde Aderinto and Hua Li. «Ocean wave energy converters: Status and challenges». In: *Energies* 11.5 (2018), p. 1250 (cit. on p. 6).

[11] Benjamin Drew, Andrew R Plummer, and M Necip Sahinkaya. *A review of wave energy converter technology*. 2009 (cit. on p. 6).

[12] Balazs Czech and Pavol Bauer. «Wave energy converter concepts: Design challenges and classification». In: *IEEE Industrial Electronics Magazine* 6.2 (2012), pp. 4–16 (cit. on p. 6).

[13] Judicael Aubry, Hamid Ben Ahmed, Bernard Multon, Aurélien Babarit, and Alain H Clément. «Wave energy converters». In: *Marine renewable energy handbook* (2011) (cit. on pp. 8–10).

[14] Dimitrios N Konispoliatis. «Floating Oscillating Water Column Wave Energy Converters: A Review of Developments». In: *Journal of Energy and Power Technology* 6.1 (2024), pp. 1–29 (cit. on p. 8).

[15] Paddocks Engineering Ltd. *Paddocks Engineering Ltd. - Marine Engineering Services*. Accessed: 2024-11-21. 2024. URL: `http://www.paddocks1.co.uk` (cit. on p. 8).

[16] Wave Dragon ApS. *Wave Dragon - Wave Energy Converter Technology*. Accessed: 2024-11-21. 2024. URL: `https://www.wavedragon.com/` (cit. on p. 9).

[17] CorPower Ocean. *CorPower Ocean Secures EUR 32M Series B1 Funding to Commercialise Wave Energy*. `https://corpowerocean.com/corpower-ocean-secures-eur-32m-series-b1-funding-to-commercialise-wave-energy/`. Accessed: 2024-11-22 (cit. on p. 9).

[18] WaveStar Energy. *About WaveStar Energy*. `https://wavestarenergy.com/about/`. Accessed: 2024-11-22 (cit. on p. 10).

[19] Matt Folley. *Numerical modelling of wave energy converters: state-of-the-art techniques for single devices and arrays*. Academic Press, 2016 (cit. on pp. 12–15).

[20] Aleix Maria-Arenas, Aitor J Garrido, Eugen Rusu, and Izaskun Garrido. «Control strategies applied to wave energy converters: State of the art». In: *Energies* 12.16 (2019), p. 3115 (cit. on pp. 15–17).

[21] Giorgio Bacelli and John V Ringwood. «Numerical optimal control of wave energy converters». In: *IEEE Transactions on Sustainable Energy* 6.2 (2014), pp. 294–302 (cit. on pp. 16, 18, 37).

[22] David G Wilson, Giorgio Bacelli, Ryan Geoffrey Coe, Diana L Bull, Ossama Abdelkhalik, Umesh A Korde, and Rush D Robinett. *A comparison of WEC control strategies*. Tech. rep. Sandia National Lab.(SNL-NM), Albuquerque, NM (United States), 2016 (cit. on p. 16).

[23] John V Ringwood, Siyuan Zhan, and Nicolás Faedo. «Empowering wave energy with control technology: Possibilities and pitfalls». In: *Annual Reviews in Control* 55 (2023), pp. 18–44 (cit. on pp. 16, 17).

[24] Nicolás Faedo, Fabio Carapellese, Edoardo Pasta, and Giuliana Mattiazzo. «On the principle of impedance-matching for underactuated wave energy harvesting systems». In: *Applied Ocean Research* 118 (2022), p. 102958 (cit. on pp. 17, 38).

[25] National Renewable Energy Laboratory and Sandia National Laboratories. *WEC-Sim: Wave Energy Converter SIMulator*. Accessed: 2024-12-02. 2024. URL: `https://wec-sim.github.io/WEC-Sim/main/index.html` (cit. on p. 20).

[26] Sandia National Laboratories. *WecOptTool: A Toolbox for Wave Energy Converter Optimization*. Accessed: 2024-12-02. 2024. URL: `https://sandialabs.github.io/WecOptTool/` (cit. on p. 21).

[27] Leo H. Holthuijsen. *Waves in Oceanic and Coastal Waters*. Cambridge University Press, 2007 (cit. on p. 34).